

PARTICULATE MATTER ANALYSIS BY ELECTRON MICROSCOPY

FINAL REPORT

Prepared for the California Air Resources Board

Interagency Agreement A2-058-32

December, 1984

Prepared by:

Steven B. Hayward, Walter John, Lurance Webber, and Jerome J. Wesolowski
Air and Industrial Hygiene Laboratory
California Department of Health Services
2151 Berkeley Way
Berkeley, CA 94704

Submitted to: John Holmes, Ph.D., Chief
Research Division
California Air Resources Board
P. O. Box 2815
Sacramento, California 95812
Eric Fujita, Contract Officer

DISCLAIMER

"The statements and conclusions in this report are those of the contractor and not necessarily those of the California Air Resources Board. The mention of commercial products, their source or their use in connection with material reported herein is not to be construed as either an actual or implied endorsement of such products".

TABLE OF CONTENTS

	<u>Page</u>
List of Figures	iii
List of Tables	v
Abstract	vi
I. Introduction	1
A. Background: The Need for Source Apportionment	1
B. Source Apportionment by Bulk Analysis	2
C. Source Apportionment by Automated Particle Analysis	3
D. Objectives of the Study	6
II. The Development of the AIHL/ARB Center for Automated Particle Analysis	6
A. Basic APA Methodology	6
B. Developments in Sampling and Analysis	8
C. Developments in Data Processing	14
III. Application: Cement Plant	17
A. Objective	17
B. Experimental Methods	18
C. Results and Discussion	19
IV. Summary and Conclusions	23
V. Recommendations	24
VI. Acknowledgements	25
VII. References	27
APPENDIX A	29

FIGURES (After page 34)

NUMBERS

1. SEM secondary electron image - gypsum particles on C film.
2. Binary LeMont image - gypsum particles on C film.
3. EDX spectrum of carbon stub.
4. SEM stub-holder made of nuclear grade graphite.
5. SEM image of the surface of a beryllium planchet.
6. SEM image of the surface of a carbon planchet.
7. Carbon SEM stub with "get lost" hole.
8. EDX spectra of 0.3 μ m brown glass particle.
 - a. On carbon planchet.
 - b. On thin carbon film.
9. Plot of SEM image resolution versus condenser lens setting.
10. EDX spectra of a small graufilter glass particle on a carbon film at two condenser lens settings.
 - a. 11:00 (Bright) setting.
 - b. 1:00 (Dim) setting.
11. Plot of the logarithm of net peak x-ray counts versus the logarithm of particle diameter for graufilter glass.
12. Size distributions of glass particles detected by APA at 200x and 2000x magnification showing the overlap necessary for scaling.
13. Elemental peak regions of clinker particle spectrum before background subtraction.
14. "Background" regions of clinker particle spectrum before interpolation, smoothing, and false peak removal.
15. Smoothed, interpolated background spectrum of clinker particle before peak removal.
16. Net elemental peaks in clinker spectrum after subtraction of smoothed background (before removal of peaks from background).

17. Net elemental peaks in clinker spectrum after subtraction of peak-corrected, smoothed background.
18. Map of Davenport with sampling sites marked.
19. Composition of iron ore source material by APA.
20. Composition of laterite source material by APA.
21. Composition of limestone source material by APA.
22. Composition of shale source material by APA.
23. Composition of coal source material by APA.
24. Composition of clinker source material by APA.
25. Composition of cement source material by APA.
26. Composition of upwind aerosol (first sampling day) by APA.
27. Composition of upwind aerosol (second sampling day) by APA.
28. Composition of downwind aerosol (first sampling day) by APA.
29. Composition of downwind aerosol (second sampling day) by APA.
30. Composition of downwind aerosol (second sampling day-duplicate filter section) by APA.

TABLES

	<u>PAGE</u>
1. "Graufilter" glass composition as determined by quantitative energy-dispersive x-ray spectrometry of a smooth fragment in the SEM.	33
2. Brown glass composition determined by same method.	34

ABSTRACT

The AIHL/CARB Center for Automated Particle Analysis (CAPA) has been established for the development of airborne particle source apportionment techniques. An automated scanning electron microscope with energy-dispersive x-ray analysis is used to characterize individual particles based on their morphological and chemical characteristics.

During the initial phase of development at CAPA, sampling and analytical hardware was optimized. Preliminary steps in software development centered around data transfer and spectral processing, coupled with conceptual development of Distribution Analysis, which will ultimately be used for source apportionment. Sampling and analysis techniques were tested on a simple system: bulk source and upwind and downwind ambient air samples from a cement plant on the California coast. Preliminary results demonstrate that much valuable information is available from automated particle analysis. However, it will be necessary to develop more sophisticated data processing procedures. This development is ongoing at CAPA.

I. Introduction

A. Background: The Need for Source Apportionment

In the past ten years, source apportionment methods have played an increasingly important role in the study of air pollution problems. The need for controlling levels of total or respirable particulate matter in ambient air is balanced by financial constraints. As a result, research has focused on finding the most cost-effective control measures, i.e. the controls that will result in the largest decrease per dollar spent of some measureable quantity such as respirable particle mass. For this minimization problem to be solved, control measure costs must be known. But also the contribution of all the important sources to the ambient air particle mix must be determined. Thus the need for source apportionment is evident.

Source apportionment can also be useful for solving problems of more immediate public concern. Often specific emitters become targets of public scrutiny, and government agencies are requested to determine if these emitters are important sources of particulate matter in the local airshed. This situation occurs when people living in an airshed are disturbed by large quantities of fallout, either out of concern for health, or because the fallout is causing property damage or soilage. Again, source apportionment can help responsible officials understand the cause of such problems, and then measures can be taken to control such problems.

The two major types of source apportionment techniques, dispersion methods and receptor methods, complement each other. Both methods use physical measurements and mathematical models that attempt a simplification of the complex physical processes that occur in the atmosphere in order to quantify the major contributors to ambient pollutant levels. Dispersion methods use source inventories along with mathematical models of pollutant dispersion to calculate these ambient contributions. Receptor methods, on the other hand, utilize measurements of the physical and chemical characteristics of the ambient pollutants at some receptor site(s) and of source materials, along with a simple (usually linear) mathematical model, to calculate contributions of the sources to the

ambient mix. The dispersion approach has met with limited success, and has been found to be most accurate in predicting gas rather than particle concentrations, since the transport properties of particles under various meteorological conditions and the chemical reactions during transport are poorly understood. The receptor approach, on the other hand, is difficult to test independently of a dispersion model coupled with an extensive emission inventory. Despite this weakness, different receptor models have produced very similar apportionment profiles with the same data sets.

B. Source Apportionment by Bulk Analysis

Most receptor models for source apportionment have used bulk chemical analysis of particulate air samples. Mass concentrations have generally been apportioned by total weight percent to a few source categories (1, 2, 3, 4). Such studies have occasionally used particle size segregation in their calculations (5, 6, 7). Since chemical compositions of individual particles are mixed when bulk analysis is used, two assumptions are inherent in receptor models using these methods. The first assumption is that contributions of sources combine linearly at the receptor without modification, and the other is that bulk chemical analysis of the ambient sample produces a result which corresponds to a linear combination of bulk analyses of individual source samples. The extent to which these assumptions are violated will determine the validity of calculated values of source contributions.

The first assumption is violated if significant particle fallout occurs between one or more sources and the receptor, or if gaseous compounds are adsorbed on particle surfaces, both of which occur commonly in real world situations. High resolution in size selection during sampling is required if correction for these phenomena is to be attempted. The second assumption is not generally valid for current bulk analysis methods. For example, x-ray fluorescence methods are prone to systematic errors that vary according to the relative homogeneity (or heterogeneity) of particle type and chemical composition. These errors will therefore be different for ambient and source sample analysis. Other bulk methods that rely upon chemical extraction are prone to errors due to incomplete extraction.

Another limitation of bulk methods is due to the fact that particles are not uniform in size. The largest particles (often the least numerous) in any segregated size range influence the results strongly. For example, one 10 μm (physical diameter) particle contributes the same mass as $\sqrt{1000}$ 1 μm particles. It is precisely the inhalable size range ($\leq 10 \mu\text{m}$ aerodynamic diameter) for which x-ray emission analysis (one of the most commonly used techniques) is most prone to systematic errors. This is due to x-ray absorbance during passage out of the particles, which depends strongly on the energy of the x-rays, and thus on the elements producing the x-rays.

C. Source Apportionment by Automated Particle Analysis

Another method of receptor-based source apportionment involves microscopic analysis of individual particles sampled from the aerosol. Analysis by optical or electron microscopy has contributed much information about the morphology and chemical composition of these particles. Since many particles must be analyzed to achieve statistically meaningful results, the major disadvantage of microscopic analysis has been the inordinate amount of time spent on a sample by the microscopist. However, recent advances in technology have made rapid automatic microscopic analysis possible. A scanning electron microscope (SEM), controlled by an image analyzer, with energy dispersive x-ray (EDX) analysis can detect particles and measure their size, shape, and elemental composition automatically. This process, herein called Automated Particle Analysis (APA), requires only a few seconds for each particle (8).

The principal deficiencies of bulk analysis methods can be overcome by APA. Since analysis is particle-by-particle, the results do not depend on the total mix of particles. Each particle can be characterized according to size, shape, and elemental composition, all of which depend on the source of the particle. Particles can be sorted into classes, and the number of particles in each class can be expressed as a fraction of the total. Mass concentrations can be estimated based on two assumptions: 1) the thickness of a particle is equal to the width of its two dimensional projection; and 2) the density of a particle is approximated by the measured

composition of heavy elements and a concentration of light elements estimated from the ratio of background to peak counts in the x-ray spectrum.

In fact, the measured "elemental composition" of particles will vary from the true composition as a function of particle shape and size as explained in the last section. However, since the shape and size are known, the measured composition can in theory be corrected. A simpler approach is to regard shape, size, and measured composition as variables describing each particle. These variables should then vary in the same way for a set of source particles and for the ambient particles due to that source.

Once the mass and three dimensional shape of a particle has been estimated, its aerodynamic diameter can be calculated (8). The particles in a given source class can then be expressed as number or mass percent of any specified aerodynamic size fraction.

When ambient particles fall into a few very distinct classes that have widely separate characteristics, the sorting can begin by inspection of single ambient particle data or by inspection of data on source particles. Use can then be made of the software available from LeMont Corporation (the manufacturer of AIHL's image analyzer), which performs a linear categorization based upon specified bounds of the particle characteristics. For example, if the particles are expected to fall into two major classes: iron particles, and cement particles, the two sets of bounds might be 1) all particles with greater than 95% of all net x-ray counts as iron (Fe) x-rays, and 2) all particles with calcium (Ca) x-ray counts greater than 55% and less than 75% of the net x-ray counts, and silicon (Si) x-ray counts between 25 and 40% of the net x-ray counts. There is obviously no overlap between these two categories, and any particles not fitting into either category would be classified "miscellaneous". The LeMont software would test the particle to see if its characteristics fit within the bounds specified for iron particles, and if not, it would test to see if it fit into the cement particle bounds. One level of subclassification

within each category is also possible. For example, iron particles could be subclassified according to whether they were respirable (aerodynamic diameter D_a less than 3.5 microns) or not ($D_a > 3.5 \mu\text{m}$).

In cases where many types of particles are present, the LeMont categorization method becomes extremely clumsy. In fact, if there is significant overlap between particle types, or if there is wide variation within types, it becomes impossible to use this simplified technique.

We have developed a theoretical method for fitting particles from an ambient mix to several sources if source samples can be obtained. This method, which we call Distribution Analysis, is potentially very powerful, although it has yet to be fully implemented. The theory is described in some detail in Appendix A, and initial steps toward implementation are described under Data Processing Developments below.

Among the important factors which define a particular APA are:

- The methods used for sample collection and preparation,
- The nature of the substrate used for analysis,
- The parameters of electron microscope operation,
- The extent to which instrument artifacts reduce the analytical accuracy,
- The manner in which shape, size, and spectral information is processed,
- The way standard source samples are obtained and prepared for analysis, and
- The sophistication of methods used for categorizing particles.

The success or failure of APA in solving a given source apportionment problem will depend on all of these factors. This report will discuss progress in all of these aspects of APA as carried out at the AIHL/ARB Center for Automated Particle Analysis (CAPA).

D. Objectives of the Study

The objective of this study was the development of a powerful new method for the identification of sources of airborne particulate matter and the apportionment of the contribution of each source to the total particulate loading in community air. The method was to be based on the morphological and elemental analysis of single particles by an automated particle analysis system.

Much progress has been made toward these objectives. Developments necessary for APA, including improvements in sample collection and preparation methods, optimization of electron microscope operating parameters, and elimination of instrument artifacts, have been successfully completed. Progress had been made in the data processing necessary to implement Distribution Analysis, a powerful new method for particle source apportionment. Finally, application of the sampling and analysis techniques to a simple system suitable for a first treatment by LeMont's software has been completed.

II. The Development of the AIHL/ARB Center for Automated Particle Analysis (CAPA)

A. Basic APA Methodology

This section describes the basic APA methodology as it was available when CAPA was first established. In the system in use at AIHL/CAPA, the computer controlling the SEM beam has the choice of two signals to make a (binary) particle/no particle decision: the secondary electron signal, and the backscattered electron signal. The secondary, or low energy orbital electrons are produced copiously in most samples. However,

differences in their numbers result mostly from surface features (roughness). Backscattered electrons, which are essentially high energy incident electrons that have been Rutherford scattered by nuclei, are much less numerous, especially within the solid angle subtended by a typical detector. Differences in backscattered signals are caused by differences in atomic numbers rather than by surface features.

Previous research by APA on air particles has usually used the backscattered electron signal to detect particles on a Nuclepore filter based on the assumption that their average atomic number would be higher than that of the filter. The fact that this method precluded the detection of particles made up principally of light elements was thought to be of little consequence, since the coarse fraction from a dichotomous sampler was usually the sample of interest (11). If on the other hand the secondary electron signal is used for particle detection, so that all particles are detectable, which is the approach taken in the present work, the substrate must be virtually featureless (free of "roughness" features that can be mistaken for particles). Furthermore, an algorithm is required to prevent the artificial breaking up of the image of a particle due to lack of secondary electron contrast in the (often flat) particle center.

In the LeMont system, particles are detected by establishing a signal threshold (either secondary or backscattered electrons) which represents a delineation between particle and background. Figure 1 is a typical gray-scale secondary electron image, while Figure 2 is a binary image (features above the threshold are white while those below are black). The beam is scanned under computer control until a particle (signal above threshold) is encountered. The beam is then moved systematically within the particle until the perimeter points are located. Once the locations of these points are stored and the center of mass of the particle is computed, the beam is positioned to acquire an EDX spectrum from the particle.

The method of positioning for EDX acquisition is selected by the operator from three possible choices: single point, multipoint, and continuous scan.

In single point acquisition, the beam is positioned on the two dimensional center of mass. In multipoint acquisition, the beam is positioned on five separate points including the center of mass and four points between the perimeter and center of mass. In this case, the spectrum acquired at each position is stored separately. In continuous acquisition, the beam is scanned around within a circle between the center of mass and the perimeter, and the integrated spectrum is stored. In the present work, either the single point or continuous scan method of positioning is used.

B. Developments in Sampling and Analysis

Initial work at CAPA centered on optimizing data acquisition from individual particles. Optimization proceeded on three fronts: the modification of the scanning electron microscope (SEM) to eliminate spurious peaks in the Energy-Dispersive X-ray (EDX) spectrum, the development of sample substrates and special sampling techniques that allowed the most information to be extracted from the air particles, and the optimization of SEM and EDX operating parameters to obtain the best compromise between particle detection/shape resolution and elemental signal-to-noise ratio.

Figure 3a is an EDX spectrum obtained from a carbon stub in the standard JEOL SEM sample holder. The large continuous background that peaks at approximately 1.8 keV is mostly due to x-rays generated in the carbon stub as the electrons lose their energy due to inelastic collisions with carbon atoms. "Spurious" peaks are evident at 8.04 and 8.63 keV due to characteristic copper (Cu) and zinc (Zn) x-rays. These x-rays are generated in brass components of the sample holder, stage, and chamber, both by backscattered electrons and by background x-rays generated in the carbon. Since these peaks would interfere with Cu and Zn peaks generated by these elements in a sample particle, steps were taken to eliminate them. First, all metal components in the sample chamber and sample stage within line-of-sight of the x-ray detector were coated with liquid graphite (DAG). This step decreased the size of the peaks, but did not eliminate them. Second, a new stub-holder was fabricated out of "Nuclear" grade graphite, the purest graphite available. Figure 4 shows the sample holder, while Figure 3b shows a spectrum taken from a carbon stub mounted in this holder. Note the lack of spurious Cu and Zn peaks.

Once the x-ray background reduction was accomplished, work was initiated to select sample substrates. A TSI 3100 electrostatic precipitator (ESP) was purchased for sampling, since its collection efficiency for particles up to several microns in aerodynamic diameter (D_a) is relatively independent of D_g , and it can produce particles on a "featureless" substrate as required for APA. The initial choice of substrate, a beryllium planchet, was found not to be at all featureless. Figure 5 is an image of the planchet surface taken in the SEM. The two prominent types of features seen are straight grooves (presumably from polishing) and round inclusions. These inclusions, which are flush with the surface, contain aluminum, silicon, and other impurities. Although the grooves can sometimes be overlooked by the APA system, the inclusions are always detected and counted as particles, making these planchets unsuitable for sampling and analysis.

Carbon planchets were tried next. Figure 6 shows an SEM micrograph of a carbon planchet surface. Although the surface is far from smooth with respect to particles 0.1 μm in diameter, it is sufficiently smooth to be used to analyze particles 1 μm or greater in diameter. Unfortunately the sampling rate of the TSI electrostatic precipitator is so low that, under most ambient conditions and with sampling times less than 8 hours, the number of particles per electron microscope field with diameter $> 1 \mu\text{m}$ is extremely small even at low (200x) magnification. The exception to this occurs when there is a source of large particles nearby. Such was the case for example in an energy efficient office building which used a rockbed for heat storage. This rockbed was apparently a source of enough large particles that the TSI ESP collected a suitable number of particles for APA in one hour of sampling (9).

Since large (1-10 μm) particles could not normally be sampled effectively in a reasonably short time period with the ESP, filtration through a 0.4 μm pore size 37 mm Nuclepore polycarbonate membrane filter with a medium flow rate (≈ 15 liters/min) was tried. Nuclepore filters consist of a flat surface perforated with uniformly sized pores. Since the particles of interest are larger than the pores, the Nuclepore substrate may be used with the image analyzer which can be made to ignore any features

smaller than 1 μm , whether they be smaller particles or replicas of filter holes. Ambient samples obtained in Berkeley in 1-4 hours were found to have sufficient loadings of large particles for statistically significant numbers (several hundred) to be analyzed at low magnification in just a few frames. Unfortunately, even after carbon-coating, the filter sections observed in the SEM were sensitive to beam damage, with the result that the setting of the background threshold required constant adjustment.

To eliminate this problem, carbon-coated filters were cleared onto beryllium (Be) grids using a modified Jaffe Wick technique (10). In this technique a small section of the filter is placed on the grid, and the entire assembly is placed on a section of polyurethane foam that is soaked with chloroform. The result was a thin carbon film with the air particles embedded in it suspended across the grid. The grid was then mounted in a specially fabricated carbon stub which had a hole drilled below the grid at such an angle as to allow the beam to "get lost" (see Figure 7). The result was that the only x-rays reaching the detector were generated either in the particle itself or in the thin carbon film, which produces a much reduced background compared to a carbon stub or planchet (see below).

Having established a successful technique for the analysis of particles 1-10 μm in diameter, a similar analysis technique was developed for particles less than 1 μm in diameter. In this case, it is necessary to sample onto a featureless substrate. The ESP can be used for this, because the number concentration of fine particles is much higher than for coarse particles. Plastic-(formvar) and carbon-coated Be grids were used for sampling in the ESP, and then were re-coated with carbon. The formvar was then dissolved with dioxane vapors, and the grid was mounted in the special stub for APA.

Figure 8a shows the EDX spectrum acquired from a 0.3 μm diameter glass particle on the surface of a conventional carbon stub. The high background is due to the x-rays generated in the stub. Figure 8b shows the spectrum of a similar glass particle suspended on a carbon-coated Be grid, using the specially-drilled stub. The principal difference between

these spectra is the much improved signal-to-noise (S/N) ratio in Figure 8b due to the background reduction. Small peaks (Ca and Na) to the right and left of the strong Si peak are clearly visible above the noise in Figure 8b.

The other advantage of using carbon-coated Be grids is the featureless background, especially in the case of the ESP sampling which is used prior to analysis of small (0.05-1 μm) particles. In this case, the background is featureless well past the resolution limit of the SEM. Therefore any particles detected by the secondary electron detector will be real, and not artifacts of the sample substrate. This means that all particles can be detected, including those consisting principally of light elements, by the secondary electron detector.

Concurrent with sample substrate optimization were efforts to optimize all aspects of SEM operation. The main goal of this process was to achieve a high S/N ratio in EDX spectra without sacrificing particle detectability or the ability to determine particle shapes accurately. These two goals are often at odds. For example, the higher the beam current, the higher the EDX S/N ratio. But a higher beam current increases the spot size, resulting in poorer image resolution and ultimately in less particle detectability and less shape discrimination.

To objectively evaluate all instrument parameters affecting these aspects of the analysis, test particles were produced by grinding colored glasses into fine powders in a ball shaker. Colored glasses were used because they usually contain small amounts of heavy elements, and thus produce EDX spectra with several peaks. The most useful of these were a grey (neutral density) filter glass called "graufilter" (German for "gray filter"), and a brown glass. Table 1 shows the elemental composition of graufilter as determined by quantitative EDX analysis in the SEM assuming full oxidation of all cations. (This is a condition not likely to be strictly true because of the presence of \sim 1% chlorine.) Table 2 contains the same result for the brown glass, two particles of which were used to produce the spectra shown in Figure 8a and 8b.

The first parameter varied was the sample tilt angle. Although distortion-free imaging is only possible when the specimen is untilted, the EDX collection efficiency is much improved when the sample is tilted 36° toward the x-ray detector. This allows a more favorable takeoff angle for the surface, but on fairly equant particles this is of little consequence. The most important advantage to tilting is that the solid angle subtended by the detector can be increased drastically since it can be moved closer to the sample. For small glass particles the gain in EDX S/N ratio was impressive, so tilting was deemed worthwhile. All subsequent concentration results were corrected for the foreshortening of the scanned field. However, particle dimensions were not correctable using LeMont Software. This would be of little consequence, since the only particles where an effect would be seen are very broad, flat ones. Even in this case, the area would be reduced by only a factor of 0.8, and the perimeter by less than that. Particle shape and size data can be corrected for this distortion prior to Distribution Analysis.

One of the principal determinants of image resolution as well as EDX S/N ratio is SEM beam current, which varies with condenser lens excitation and gun bias. After the gun bias was set for maximum emission according to manufacturer specifications, the effect of condenser lens setting on image resolution was measured by taking images of an NBS Standard Reference Material for SEM image resolution, "tungsten dendrites". The finest details in the images were measured as a function of condenser lens control setting with a reticle in a portable magnifier. These resolution limits, which are probably conservative because of specimen limitations, are plotted in Figure 9. Figures 10a and 10b show EDX spectra recorded at two condenser lens settings from a small graufilter particle on a carbon film substrate. Net peak and background counts for Fe and Al were estimated in these spectra. Noise (statistical fluctuation) values were calculated as the square root of these net counts. Total noise was then calculated assuming that the peak and background noise components are independent and therefore add in quadrature. S/N ratios were calculated as the ratio of net peak counts to total noise (standard deviation in total counts). The S/N ratio for the iron peak was found to increase by a factor of 3 as the beam was changed to the brighter setting, while the

Al S/N ratio increased by a factor of 2.4. From Figure 9, it can be seen that the image resolution possible from these two settings is 0.012 μm and 0.06 μm respectively. Since the latter figure means that a particle (or particle shape feature) of that size should be detectable, the large increase in EDX S/N ratio was deemed sufficient cause to use the larger spot size. Any decrease in spot size, resulting in better detectability of particles smaller than 0.06 μm , would be useless since the poorer S/N ratio would in turn prevent useful spectral information from being obtained from such particles.

The next instrumental parameter investigated was magnification. It was expected that beam positioning for EDX acquisition at low magnifications would be less accurate than at high, resulting in reduced EDX peak counts. This turned out to be the case, as illustrated in Figure 11. The three sets of data in this figure were all acquired under the same conditions from the same glass powder sample, with one exception, the magnification. The principal difference between 200x and 2000x magnification is that the total net EDX counts (those due to the particle elemental composition) decreases much more rapidly with particle size at 200x. This is likely to be due to the fact that beam positioning is much more inaccurate during X-ray acquisition at this magnification. Interestingly enough, the results at 400x are not much worse than at 2000x. It was therefore concluded that "low magnification" analysis for 1-10 μm particles could be carried out at 400x with minimal EDX S/N degradation compared to higher magnifications, while decreasing the magnification further could significantly affect the S/N ratio for particles as large as 2 μm . Small particles (sampled by ESP) were to be analyzed at 2000x magnification.

The use of two sampling schemes and two analysis magnifications for small and large particles actually requires that some overlap in particle size be achieved in order to scale the two sets of data. The feasibility of such a scaling procedure is shown in Figure 12. Here size distributions of particles analyzed from the same sample of glass powder but at high and low (in this case, 200x) magnification are plotted. The high magnification distribution can be scaled up such that the total numbers of particles between, say, 1.5 and 2.3 μm in diameter are equal. It should be noted

that, if 400x magnification had been used instead of 200x, the low magnification curve would have extended further to the left before showing the dropoff (due to loss of analytical detection efficiency) that is evident in the graph.

C. Developments in Data Processing

As will be shown later in this report (see Application: Cement Plant), apportioning sources based on the wealth of data available from APA is a process for which LeMont software is suitable only in the simplest of cases. In situations in which characteristics of source particles overlap, techniques generally termed "pattern recognition" are required. We have developed such a technique which we call Distribution Analysis, which is described in detail in Appendix A. Although this technique has not yet been implemented computationally, we have taken several preliminary steps in data processing so that it can be implemented.

The fact that Distribution Analysis is an extremely complicated computational procedure necessitates the use of a high speed computer to implement it. The data are therefore transferred from the LeMont image analysis computer to a PDP-11/34 for processing. This transfer is accomplished by removing floppy discs from the LSI-11/23 where the data is written, and inserting them into the PDP. However, the use of different operating systems on the two computers necessitated the development of software for data translation and unpacking, as well as for processing of raw x-ray spectral and size data prior to Distribution Analysis.

In order to understand the need for x-ray spectral processing, it is necessary to first consider the limitations of current processing available from LeMont. The LeMont system stores the integrated total peak along with flanking background counts for each of approximately 30 elements monitored. The average background per channel is calculated, and then the corresponding total background in the peak area is subtracted from the peak to give net counts. This method of background subtraction is subject to two serious errors. First, when the background counts are low, the measured background value can be quite inaccurate due to statistical

fluctuations. Second, when a neighboring peak overlaps the "background" region, the background counts will be too high. These errors can be reduced by subtracting a smoothed background. The logical first step in actual data processing for Distribution Analysis is therefore background smoothing and subtraction.

After initial use of the "FLX" utility to convert data to the format understood by the PDP's operating system, data had to be translated into a format readable by LeMont routines run on the PDP by a translation program called TRANS, which was written at AIHL in Fortran. Readability by LeMont routines was necessary since the basis for the spectral and size data processing on the PDP was a core of LeMont Fortran and Macro-11 routines called a "Minimum Source Package". This package consisted of a selected set of LeMont routines necessary to interpret LeMont data files based on information written by other LeMont routines to "Chemistry Definition" files on the LeMont computer. The Minimum Source (MS) Package is the framework around which the PDP spectral and shape data processing program was written. Routines were all written in Fortran, and calls were made by the MS package to which they were linked. These routines perform the following functions:

<u>Subroutine</u>	<u>Description</u>
PLTSET	Allows operator to select spectral plot displays
WRDAT	Writes processed data to a file for Distribution Analysis
SPCPRC	General spectral processing (calls following routines)
BAKSUB	Subtracts backgrounds
WPLOT	Writes special data to a plot file for plotting
FOPEN	Attaches plot files
BFFT	Performs Fourier transforms
QINT	Interpolates spectra quadratically
BAKINT	Interpolates and smooths backgrounds

Prior to implementation of Distribution Analysis, some further particle data processing will be required in the future. This includes routines to test for variables that are not significantly different from zero (e.g., elements whose presence is due merely to background fluctuations) and to produce plots of selected two dimensional projections of the data.

III. Application: Cement Plant

A. Objective

Before APA could be used for apportioning a complex mix of sources of air particles, it was deemed necessary to apply APA techniques to a relatively simple source problem. A source of air particulate had to be found that had a very low background (minimal sources) upwind. It had to produce particles which contained enough heavy elements so that good elemental signatures could be obtained. And it had to be accessible for bulk sampling of typical source particles.

A cement plant in Davenport, CA happened to be just such an ideal source for initial testing of APA techniques. It is located just downwind of the Pacific Ocean on the California coast approximately ten miles north of Santa Cruz. The only land-based source of particulate matter upwind of the plant (during prevailing westerly wind conditions) is Highway 1, which is fairly lightly travelled at that point. Samples of likely source materials were obtainable from the plant with the permission of management. These included several types of particles with significant amounts of elements heavy enough to be detected by EDX, such as aluminum, silicon, calcium, and iron. Source emissions were of two types: stack and fugitive. Stack emissions were likely to contain clinker and finished cement, as well as certain amounts of starting materials: laterite, iron ore, shale, limestone, and gypsum. Stack emissions were also expected to include some coal fly ash, since coal was used to fire the kiln. Fugitive emissions were likely to include windblown dust from coal piles, from several piles of the starting and intermediate materials on site, and from waste cement piles on site. Fugitive emissions of these same materials were also expected from the plant itself.

B. Experimental Methods

Air samples were collected at two sites, one downwind and one upwind of the plant. Figure 18 is a map of the plant area with the two sampling sites marked. The upwind site was adjacent to an artificial salmon spawning facility near the beach west-north-west of the plant. The downwind site was on a bluff east-south-east of the plant, approximately 500 meters from the kiln stack. Filter samples for coarse particle analysis were collected on 0.4 μm pore size, 37 mm diameter polycarbonate membrane filters for approximately 3 hours. Typical flow rates were 18 liters/min at the start and 16 liters/min at the end of the sampling period. Flow rates were calibrated with a dry test meter. Samples were collected on two separate days in April during a period between 11 a.m. and 3 p.m., when the typical offshore flow was strong (20-45 Km/hour). On the first day the stack emissions were observed to pass over the downwind sampling site several times. On the second day, the wind direction was more northerly than on the first, and so the downwind site was actually somewhat downwind of a large pile of laterite on site during much of the sampling time.

ESP samples for the fine ($< 1 \mu\text{m}$) fraction could not be collected on the first day because of a sampler malfunction. On the second sampling day, most sample grids were lost as a result of the necessity of mounting and dismounting them from the sampler in the field under windy conditions. The few grids that were salvaged were badly damaged. Therefore in this study only filter air samples were analyzed. Air filter samples were carbon-coated, and the filter material dissolved by chloroform vapor in a modified Jaffe Washer.

The following raw materials were collected from piles on the plant grounds: laterite, iron dust, shale, and limestone. Coal dust was collected from the pile of coal used to fire the kiln. Clinker dust was collected from the clinker house, and finished cement dust was provided by plant personnel.

For the purposes of this pilot study, exact representativeness of filter samples was not deemed crucial. This is because the LeMont classification

software was to be used, with no information on size distributions of the raw material contributing to their classification. For this reason the following crude method of sample resuspension and filtration was deemed sufficient.

Most bulk dust samples were prepared by shaking a small amount in a plastic bag and sampling from the bag using a 0.1 μm pore size 25 mm polycarbonate membrane filter attached to the house vacuum line. These filters were then prepared in the same manner as the ambient air filter samples. In a few cases such as coal dust, static charge caused most small particles to adhere to the bag, so an alternative preparative method was used. A small amount of dust (20-130 mg) was suspended in approximately 125 ml of filtered water or ethanol and sonicated for 15 minutes. A 5 ml aliquot was drawn off and added to 25 ml filtered water or ethanol in a filter funnel. This suspension was then filtered through a 47 mm polycarbonate membrane filter (0.1 μm pore size) and prepared in a manner identical to that used for the air samples.

C. Results and Discussion

APA was carried out on all source material samples and the upwind and downwind air filter samples at 400x magnification using single-point EDX analysis. Because of the lack of fine fraction samples, particle sizes were not restricted to greater than 1 μm . The source material sample analyses were each used to establish chemical classes for source particles. Classes were first defined by inspection of particle-by-particle data. In most cases, such as iron and laterite, only one class was defined for each source type. In the case of clinker, though, several types of particles primarily of Ca and Si were observed, with the Ca/Si ratio varying from approximately 2 to 4. Three classes of these particles were established, one high Ca/Si, one low Ca/Si, and one midrange. Each set of source particle data was then classified based on the composite chemical classification scheme, using LeMont software. This allowed a rough refinement of the chemical classifications so that more of the source particles would be properly classified.

Source sample printouts using the refined classifications are shown in Figures 19-25. These show particle number percent by category. Besides the source categories (coal, "clinkers", high Ca/Si clinkers, low Ca/Si clinkers, shale, laterite, gypsum, limestone, and iron ore), the figures include more standard categories, such as NaCl/marine, feldspar, glass, etc.. The categories labeled "no counts", "low low counts", and "low counts" include particles having no net x-ray counts, 1-100 net counts, and 101-200 counts respectively. These particles are expected to be principally composed of light elements such as carbon, nitrogen and oxygen, whose x-rays were undetected. Other categories, such as iron chlorides, and calcium, are similar to but less stringent than source categories which in this case are iron ore, NaCl/marine, and limestone. For example, iron ore particles have greater than 200 net counts, at least 96% of which must be iron counts, while "iron" particles have greater than 200 net counts, at least 20% of which must be iron counts. Because of the linear nature of the classification scheme, particles are checked for inclusion in the iron ore category before they are checked against the iron category. Therefore "iron" particles can be assumed to contain less than 96% iron counts.

It can be seen from Figure 19 that 98% of all of the particles from the pile of iron ore are classified as such. Interestingly enough, of the other two percent, one percent was laterite. The iron ore pile was directly adjacent to the laterite pile. Figure 20 shows a fairly similar result: 83% of the particles sampled from the laterite pile (which was between the iron and coal piles) were so classified, while most of the rest were classified as iron ore, iron, or coal. Figure 21 shows that 84% of the particles from the limestone pile were classed limestone or calcium particles. Other particles found were laterite (4%), clinker, coal, glass (1% each), miscellaneous and miscellaneous silicate (8% combined). Most miscellaneous particles in this case tended to be of unclassified "crustal" compositions. From Figure 22 it can be seen that shale is actually a complex mixture. Of all the mineral types found in this sample, silica is the most numerous (43%), followed by miscellaneous silicates (30%), shale (11% - the largest group of well-defined non-silica particles), mica-vermiculite (4%), laterite and miscellaneous (3% each), and coal and limestone (2% each).

Figure 23 shows that coal is contaminated with several minerals, a result which is not at all surprising. The coal category is based on the ratio of net counts to total background counts, which is low for coal because of its high carbon content, and therefore there is potential here for misclassification of other low-Z particles. Figure 24 shows another fairly complex mixture in clinker dust, although again the components are reasonable. 43% of the particles are classified as clinker, 16% as limestone or calcium, 12% as coal, 12% as miscellaneous and miscellaneous silicates (40-90% silicon, all other elements less than 20%), 11% as "no count" particles, and small amounts as laterite, iron ore, iron, and various other minerals. The finished cement is much cleaner, as shown in Figure 25. 68% of the particles are classified as "clinker", and 26% as miscellaneous. The rest are gypsum, limestone and calcium, laterite, and talc. Of the miscellaneous particles, most contain Ca, S, and Si in descending order, but with widely varying composition. A future "cement" category will attempt to classify these particles. In general, however, the final classification scheme used to obtain Figs. 19-25 was effective in that it classified starting and intermediate materials in a manner consistent with their known identity.

Upwind and downwind air samples were then classified using LeMont software with the same chemical classification scheme. Results from the filter samples are summarized in Figures 26-30. Figure 26 shows the upwind results from the first sampling day. The particle concentration in the size range measured was 1×10^5 particles/m³. With the exception of 3% iron ore and 28% "coal" (the latter of which are likely to be small, low-Z particles), the results are consistent with particle contributions from sand (silica, aluminum) surface soil (shale, gypsum, mica, misc. silicates, mics.) and sea salt (NaCl, chlorides). Figure 27 shows similar results from the second day during which the wind speed was higher than on the first day. Here the particle concentration in the size range measured was 1.5×10^5 m⁻³, which is 50% higher than that measured on the first day. The second day's profile is similar to the first day's, with the exceptions being the lack of aluminum and iron containing particles, and the increase in illite, mica-vermiculite, and misc. silicate.

Data shown in Figure 28 (downwind, first sampling day) represent 5.45×10^5 particles/m³, or approximately 5.5 times the particle concentration of Figure 26. Iron and iron ore particles make up 22% of the total, while limestone and calcium (18%), clinker (15%), and laterite (5%) are the other important particles directly traceable to the plant. Miscellaneous silicate and miscellaneous particles have both increased by a factor of 5 to 7, while NaCl particles do not appear at all. Shale has increased by a factor of 5, and gypsum has increased fourfold. However, the presence of 2.5% illite, which is present only in small amounts in a few source materials, suggests that some of the downwind particles are due to windblown surface soil originating near the plant site.

Figure 29 shows downwind results for the second day. Here the particle concentration was 3×10^5 m⁻³, so the ratio of downwind to upwind concentrations is only 2:1, while the concentration is just over half of the first downwind sample. These differences are likely to have been due to the fact that the sampler was directly in the kiln plume for a significant fraction during the first day's sampling. This time, laterite is the most numerous particle, consistent with the different wind direction, while clinker, iron ore, iron, and limestone particles are all lower than in Figure 27. Again, NaCl is virtually absent, while illite, mica-vermiculite, shale, and silica are all higher than upwind.

Figure 30 is a repeat analysis of the downwind sample from the second day using another portion of the filter. The particle concentration is the same to within 2% and the particle category percentages are remarkably similar. Approximately 700 particles were analyzed to produce the data in each of these two figures, so the reproducibility is as good or better than random count statistics predict.

Both advantages and disadvantages of the currently available software for classification are illustrated by these results. Clearly many of the cement plant particles were differentiated from the natural background. If all categories had represented unique particle classes from single sources (as do the categories "iron ore" and "laterite"), then the particles in the downwind air sample could have been unambiguously apportioned. Even

if each source produced particles of several categories, these source "signatures" could be fit to the ambient mix by a least-squares method. This is actually the method sometimes called "chemical class balance" (11). However, since the assignment of a particle to a class depends on the order of the class definitions, the classes are not necessarily unique. For example, many "coal" particles would be classified "low count" particles if the coal category were placed lower on the list. What is really required is a method for segregating particles with like characteristics from a mix. This is actually one of the purposes of Distribution Analysis. But in this simple case of an isolated source, chemical categories sufficed to identify particles, so the full power of the method including particle size and shape parameters was not needed.

IV. Summary and Conclusions

Since the establishment of the AIHL/ARB Center for Automated Particle Analysis (CAPA), the development of new techniques for air particle source apportionment have included the following:

- Sampling and analysis techniques and substrates have been developed to allow all particles in each of two important size ranges to be detected and characterized with optimal x-ray acquisition
- Unique SEM components developed at CAPA have resulted in particle EDX spectra that have drastically reduced backgrounds and are free of instrument artifacts, and
- SEM operating parameters have been optimized for both particle detectability/shape discrimination and EDX spectrum S/N ratio.

Data processing development has resulted in more sophisticated data treatment methods than are currently available from instrument vendors. Initial development has centered around data transfer and translation for processing on a PDP-11/34. Data processing routines written so far are designed to extract

elemental composition and shape information from spectral and shape summaries stored by LeMont routines. This processing is capable of producing much more accurate compositional data than is obtained with LeMont software.

Finally, sampling and analysis of particles from one relatively simple source, a cement plant, was carried out in order to anticipate and overcome real world sampling problems and to test the usefulness and versatility of the LeMont software for particle classification. APA of source material and air samples from the cement plant was successful in attributing most of the downwind aerosol to plant stack and fugitive emissions. This pilot study was also valuable in solving sampling problems prior to a full scale source apportionment effort.

Analysis by LeMont software illustrated the power of the single particle approach when particles differ drastically. However, it also exposed the inability of simple linear classification methods to deal with particles whose chemical and shape characteristics vary in a continuous way. Such difficulties will be solved by the application of more sophisticated pattern recognition methods such as Distribution Analysis, the theoretical basis of which was developed as part of this work.

V. Recommendations

Clearly further work needs to be done to make APA suitable for general use in source apportionment of complex mixes of ambient air particles. Since APA hardware is now optimized, future work falls into two general categories: widespread source sampling for determination of source signatures, and computer programs for pattern recognition such as Distribution Analysis.

Work on sampling techniques should extend to all important sources within an airshed. It should include sampling at increasing distances from the sources and simultaneous measurement of windspeed and direction. Source samples for fine fraction analysis should be collected with separate upwind and downwind ESP samplers, allowing grids to be mounted and dismounted from the sampler in the laboratory. This will prevent the grids from being blown away, broken, or contaminated on site.

In the case of collection of bulk samples such as soil, road dust, or dust piles at some source, sample preparation should include the use of a fluidized bed before collection of ESP or filter samples.

Work on software development should concentrate on taking processed spectral and shape/size data from the modified LeMont Minimum Source Package, choosing significant variables, and implementing Distribution Analysis on these variables. First attempts should assume no modification of source distributions. Future work should refine the apportionment methods by evaluating residuals of the fit of source distributions to the ambient air distribution and interpreting these residuals in terms of missing sources and modification of known sources.

These tasks are clearly formidable, especially the computer programming necessary for Distribution Analysis because of the complexity and detail of data made available by APA. This mass of data from thousands of particles, each characterized by forty or fifty variables, is both a blessing and a hindrance. It is a blessing because so much detail is present, but without an operational version of Distribution Analysis it is a hindrance because current statistical methods used for source apportionment, such as multivariate factor analysis, cannot be used for a full source apportionment using APA data. Instead, techniques such as Principal Component Analysis can be useful when applied to source data to suggest the number of important subcategories within that source type and to estimate an "average" composition of each of those subcategories. It can also be used in much the same way with ambient data. However, even if those subcategories are matched to those in the sources, the "loadings" on each of these "factors" will not be related to that category's contribution to the ambient mix. Quantitation of that contribution, as well as correction for modifications to the particles and their size distributions, will still have to be accomplished by Distribution Analysis.

VI. Acknowledgements

We thank Roy Kester and Andrea Berry for help with sample preparation, Dr. Michael Tarter for discussion of mathematical aspects of Distribution Analysis,

and Kenneth Kitts of Monterey Bay Unified Air Pollution Control District for invaluable sampling assistance. We also thank Dr. Douglas Lawson and Eric Fujita for their suggestions.

This report was submitted in fulfillment of Interagency Agreement #A2-058-32, Particulate Matter Analysis by Electron Microscopy by the California Department of Health Services under the sponsorship of the California Air Resources Board. Work was completed as of December 31, 1984.

REFERENCES

1. Cooper, J.A. and Watson, J.G. (1980) "Receptor Oriented Methods of Air Particulate Source Apportionment", J. Air Pollution Control Assoc. 30, 1116.
2. Giauque, R.D., Goda, L.Y. and Brown, N.E. (1974) "Characterization of Aerosols in California by X-ray Fluorescence Analysis", Environ. Sci. Technol. 8, 436.
3. Miller, M.S., Friedlander, S.K. and Hidy H.M. (1972) "A Chemical Element Balance for the Pasadena Aerosol", J. Colloid and Interface Sci. 39, 165.
4. Wesolowski, J.J., John, W. and Kaifer, R. (1973) "Lead Source Identification of Multielement Analysis of Diurnal Samples of Ambient Air", in Trace Elements in the Environment, ed. Kothny, E.L., Am. Chem. Soc., Washington, D.C.
5. Dzubay, T.G. (1980) "Chemical Element Balance Method Applied to Dichotomous Sampler Data", Ann. New York Acad. Sci. 338, 126.
6. Gatz, D.F. (1975) "Relative Contributions of Different Sources of Urban Aerosols: Application of a New Estimation Method to Multiple Sites in Chicago", Atmos. Environ., 9, 1.
7. Lewis, C.W. and Macias E.S. (1980) "Composition of Size-Fractional Aerosol in Charleston, West Virginia", Atmos. Environ. 14, 185.
8. Casuccio, G.S., Janocke, P.B., Lee, R.J., Kelley, J.F., Dattner, S.L. and Mgebroff, J.S. (1983) "The Use of Computer Controlled Scanning Electron Microscopy in Environmental Studies". J. A.P.C.A. 33:10, 937-943.
9. Hayward, S.B., Sexton, K., and Webber, L.M. (1984) "Application of Automated Particle Analysis to Indoor Source Apportionment", Proceedings of the 77th Annual Meeting of the Air Pollution Control Association, San Francisco, 84-33.8.

10. Samudra, A.V., Harwood, C.F., and Stockham, J.D. (1978) Electron Microscope Measurement of Airborne Asbestos Concentrations - A Provisional Methodology Manual, U.S. EPA-600/2-77-178, Environ. Sci. Res. Lab, U.S. Environmental Protection Agency, Research Triangle Park, NC.
11. Johnson, D.L. and McIntyre, B.L. (1983) "A Particle Class Balance Receptor Model for Aerosol Apportionment in Syracuse, N.Y.", U.S. EPA-600/0-83-103, Environ. Sci. Res. Lab., U.S. Environmental Protection Agency, Research Triangle Park, NC.

APPENDIX A

DISCUSSION OF THE THEORY OF SINGLE PARTICLE DISTRIBUTION ANALYSIS

Although the mathematics required for a complete description is complex, this section will attempt to describe in a comprehensible way the principles of this analysis, and the practical applications based on these principles.

A. The nature of single particle data

Automated particle analysis of a particular air particle results in the generation of many numbers which describe that particle. These include several measures of shape and size (e.g., perimeter length, area, particle length and width, etc. or alternatively, selected values of Fourier shape descriptors.), as well as numbers that describe the x-ray fluorescence spectrum (such as the percentage of net peak counts due to iron, silicon, calcium, etc., as well as numbers describing the x-ray spectrum background). If the total number of these data variables describing each particle is N , then the particle can be represented as a point in an N -dimensional space. The value of the m^{th} variable determines the point's coordinate along the corresponding m -axis. In mathematical parlance, any particle can be represented as a vector in R^N , the N -fold space of real numbers.

B. Source distributions

The total ensemble of particles emitted by a source will have a "distribution" in R^N . This means that if one samples the source particles, the probability that a particle represented by a point in R^N will be found is equal to the value of this distribution. For a source that is emitting very homogeneous particles, that is, one "type" of particle, this distribution will look like an N -dimensional Gaussian "cloud" centered around some point. The coordinates of this point will represent the average values of the variables of all particles emitted by the source. If several types of particles are emitted, the distribution will consist of several "clouds", possibly overlapping, with one cloud for each type of particle.

C. Effects of processes occurring during dispersion

Modifications of the ensemble of source particles during transport to the receptor can be represented by suitable modifications of the source distribution. Agglomeration of similar particles can be represented to a first approximation by shifts in distributions along shape and size axes, although further refinements require shifts in elemental composition due to size-dependent x-ray absorption. Heterogeneous particle agglomeration can be represented in an analogous way. It should be noted that any agglomeration will result in a reduction of total integrated area under all distributions, since it results in a reduction of the total number of particles. Large particle fallout also results in a reduction of the area under the distributions, but in this case the reduction is at the large particle end of each distribution cloud. Adsorption of chemical species results in distribution shifts which vary predictably with particle shape and size. For example, SO_2 adsorption shifts distributions toward higher values along the sulfur axis, while hydrocarbon and nitrogen oxide adsorption produces shifts towards higher spectral background counts and toward different background shapes.

D. Ambient air - methods of computing distributions

Distributions can be estimated computationally from the group of points representing the particles actually sampled in air. Methods for such estimation can be parametric or non-parametric. Parametric methods require a mathematical model of the distribution, and therefore require some prior knowledge. Non-parametric methods require no such model. Since they assume nothing about the distribution shape, these methods require many data points (particles) to be sampled before a good estimate of the distribution can be obtained. Since automated particle analysis can easily result in data from 500-1000 particles from one sample, non-parametric estimation is the method of choice. In particular, we have chosen "kernel density estimators" for our non-parametric computations because they are suitable for many-particles and many-variables.

E. Fitting unmodified source distributions to ambient distributions

The particle distribution at the receptor site is simply the sum of all source distributions weighted by the extent each source contributes at the receptor to

the total particle mix. Although for correctness the source distributions should be modified by the processes that occur during transport (as described in the last section), in the first step in the analysis we can assume no such modification. Our task then becomes that of estimating the particle distribution at the receptor (by non-parametric methods) from the ambient sample data, and fitting a sum of weighted source distributions to the receptor distributions by a least-squares procedure. Further refinements to account for non-linearities are described below.

F. Looking for modifications of source distributions

The fitting procedure described above will result in weights for source distributions. For some sources these weights may be zero, which means that the contribution of these sources at the receptor is negligible. If one calculates the sum of weighted source distributions and subtracts this from the receptor distribution, one obtains a residual (whose squared sum was minimized in the fitting process). The structure of this residual will contain clues as to the nature of the modifications of the source distributions that will produce a best fit to the receptor data (non-linearities). Mathematical methods exist for testing the residual for source peak shifting (adsorption and fallout), addition (agglomeration), and for the existence of unaccounted for peaks (unknown sources). Of these techniques, correspondence analysis allows the visualization of significant projections of the N-dimensions into 2-dimensions so that features can be visually discriminated, while cluster analysis allows hierarchical ordering of groups of points in these "subspaces".

G. Data for estimating source distributions

Ideally the source distribution of a point source should be estimated by sampling in the plume just downwind of the source. If this is not possible, several samples may be taken at varying distances downwind of the source. The distributions estimated from the data obtained from each of these samples should consist of a background component, and a component due to the source whose contribution will decrease with distance from the source. It is therefore possible to calculate this variable component.

Bulk material from an area source or a point source (such as a stack sample), may be placed in a fluidized-bed to generate an aerosol. This aerosol can then be sampled and analyzed in the same way as the ambient samples.

TABLE 1. "Graufilter" glass elemental composition by energy-dispersive X-ray Analysis

Element	Weight Percent	Assumed Oxide Formula
Aluminum	1.95	Al_2O_3
Silicon	36.21	SiO_2
Chlorine	1.23	Cl
Potassium	8.47	K_2O
Iron	3.05	FeO
Zinc	2.81	ZnO
Oxygen*	46.28	

*Determined by stoichiometry

TABLE 2. Brown glass elemental composition by Energy-dispersive X-ray Analysis

Element	Weight Percent	Assumed Oxide Formula
Sodium	8.27	Na ₂ O
Magnesium	0.82	MgO
Aluminum	1.46	Al ₂ O ₃
Silicon	35.44	SiO ₂
Calcium	6.38	CaO
Oxygen*	47.64	

*Determined by stoichiometry

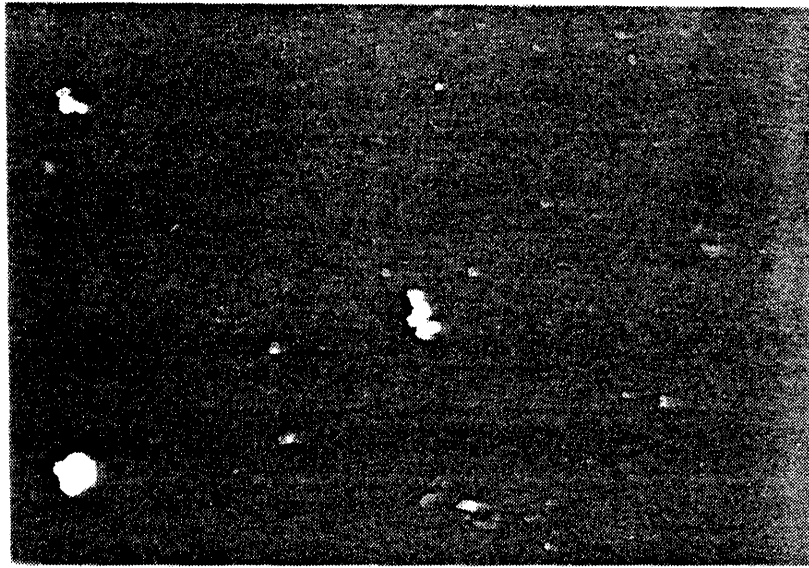
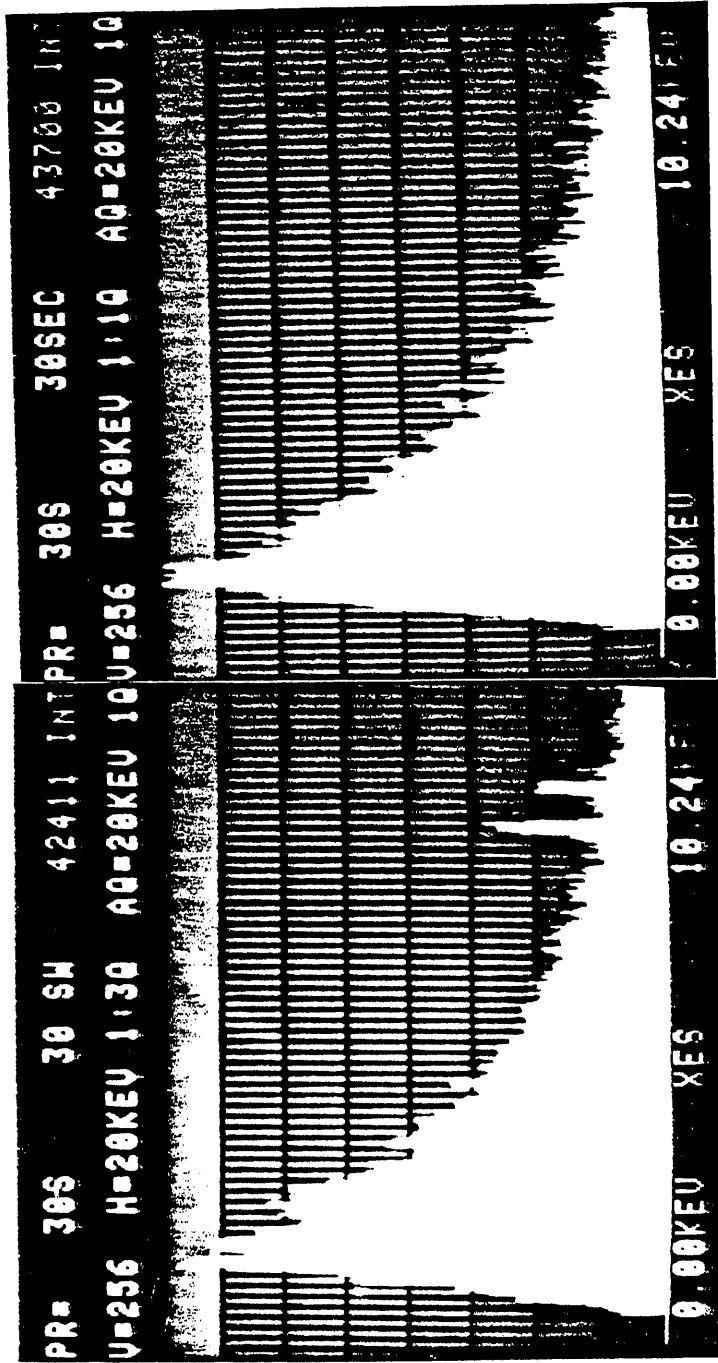


Figure 1: SEM secondary electron image-
gypsum particles on C film



Figure 2: Binary LeMONT image- gypsum
particles on C film
Scale: 1 in = 5 μ m



a. Brass stub holder

b. Nuclear-grade graphite holder

Figure 3: EDX spectrum of carbon stub

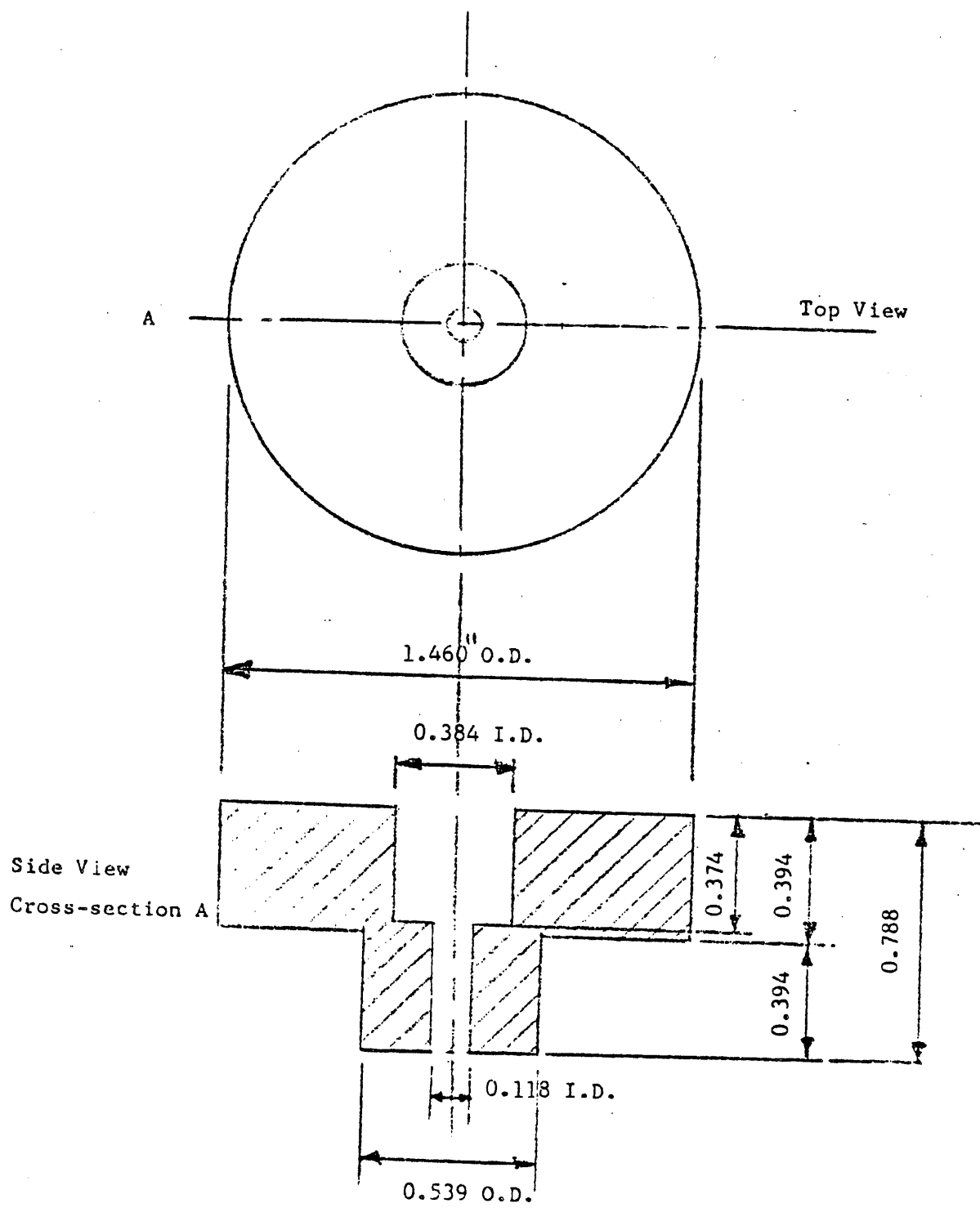


Figure 4: SEM Stub-holder made of nuclear grade graphite

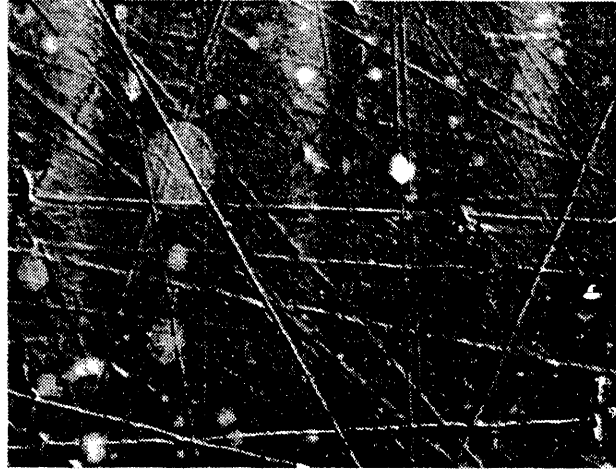


Figure 5: SEM image of the surface of a beryllium planchet
Scale: 1 cm = 2 μ m



Figure 6: SEM image of the surface of a carbon planchet
Scale: 2 cm = 5 μ m

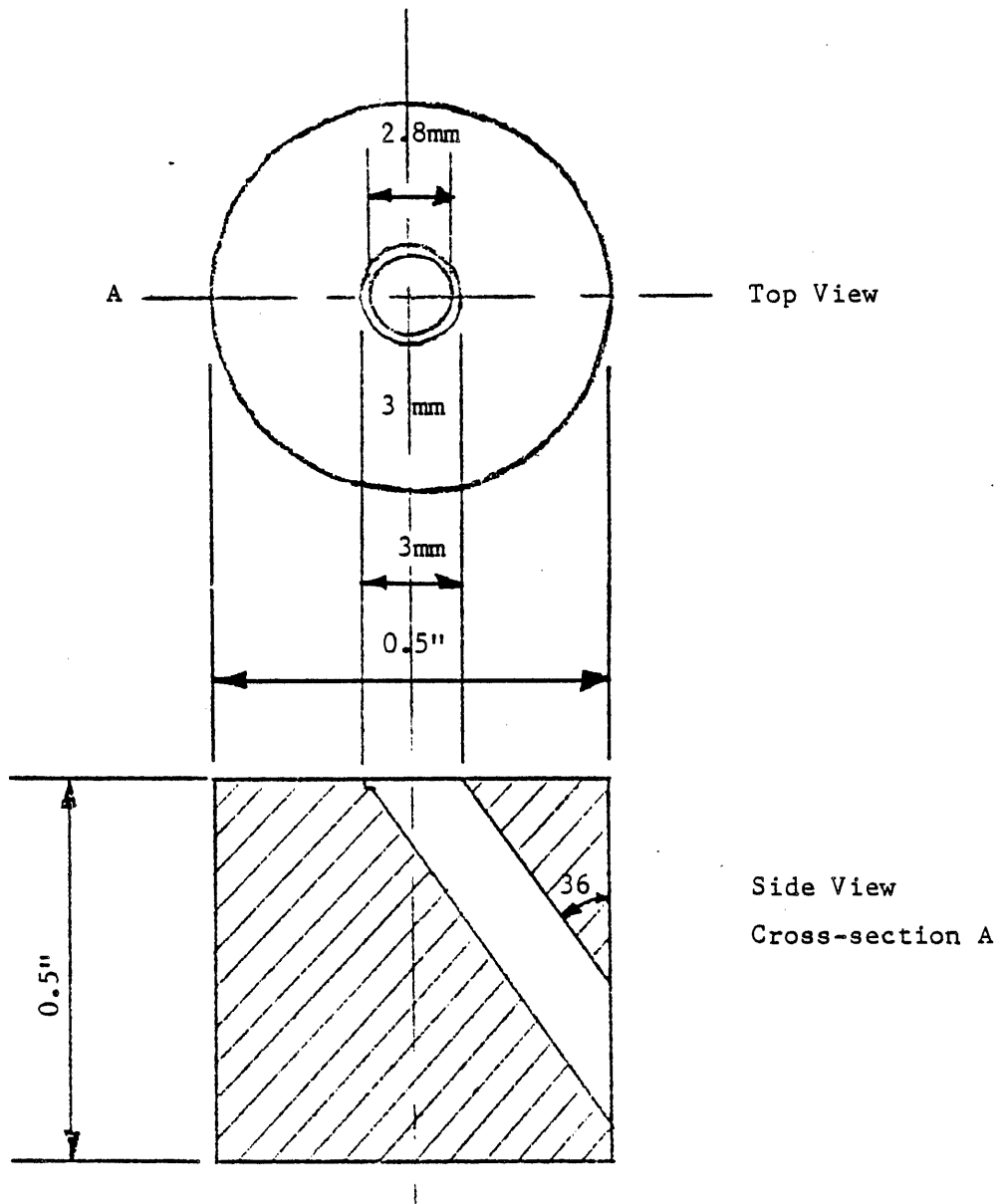
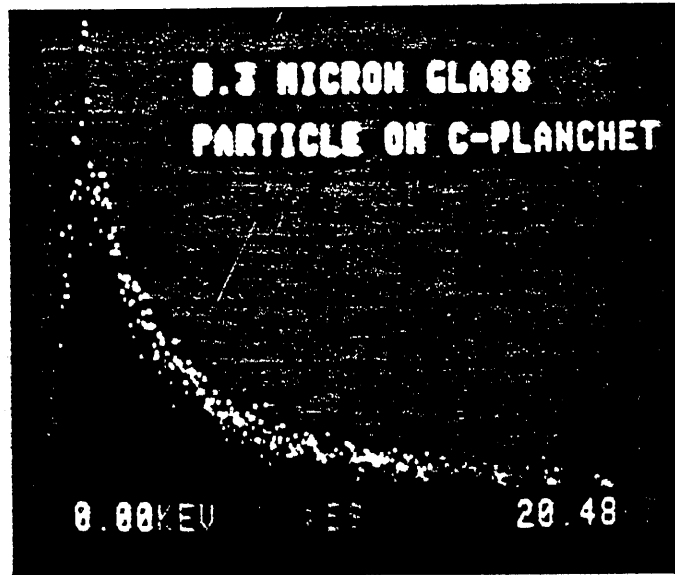
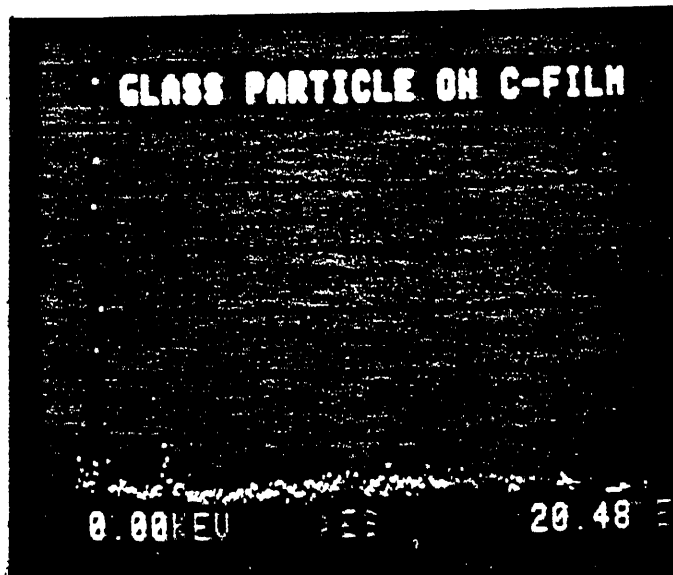


Figure 7: Carbon SEM stub with "get lost" hole.
 Stub is tilted so that the beam goes
 straight into the hole.



a. On carbon planchet



b. On thin carbon film

Figure 8: EDX spectra of 0.3 μm brown glass particle

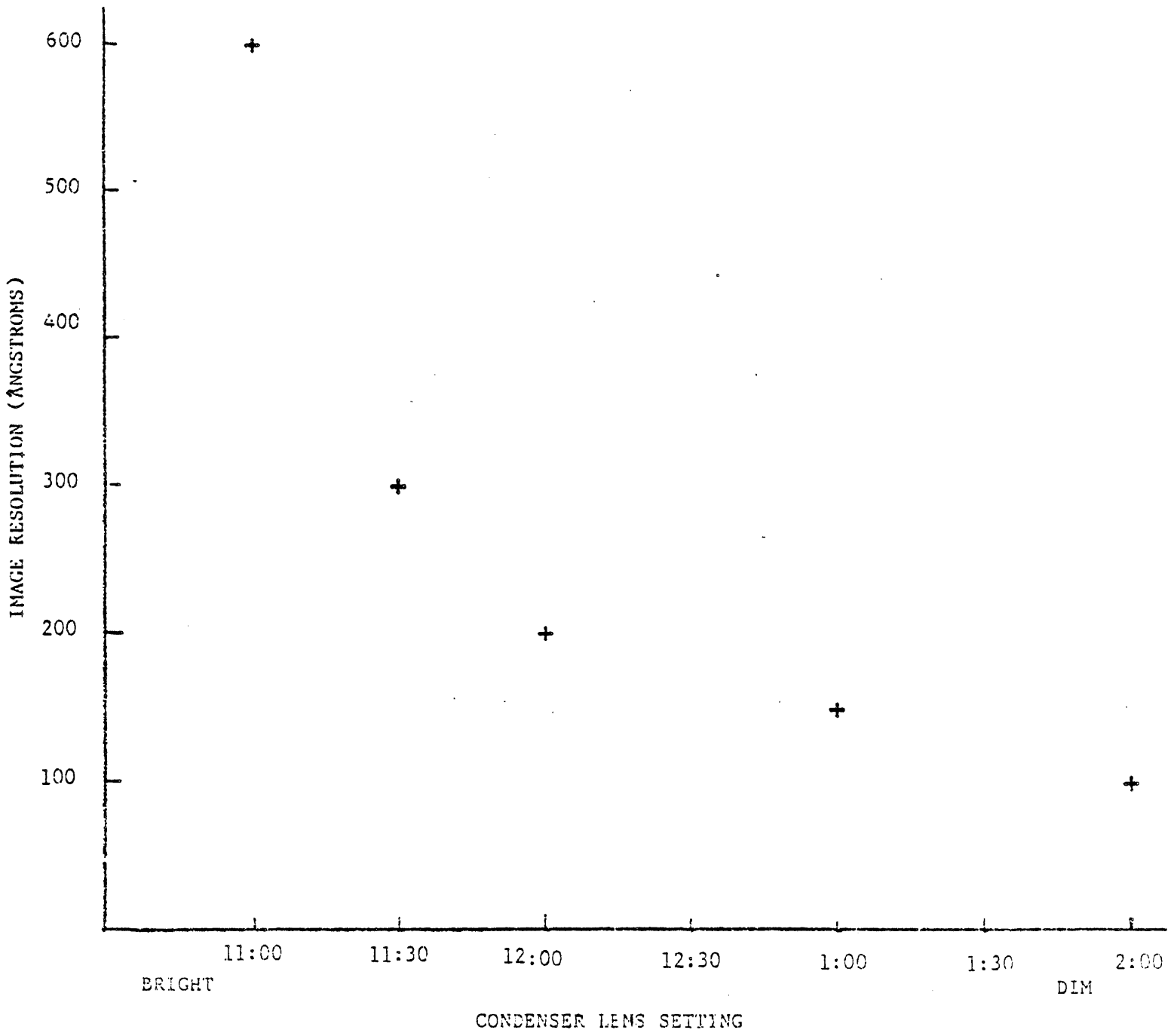
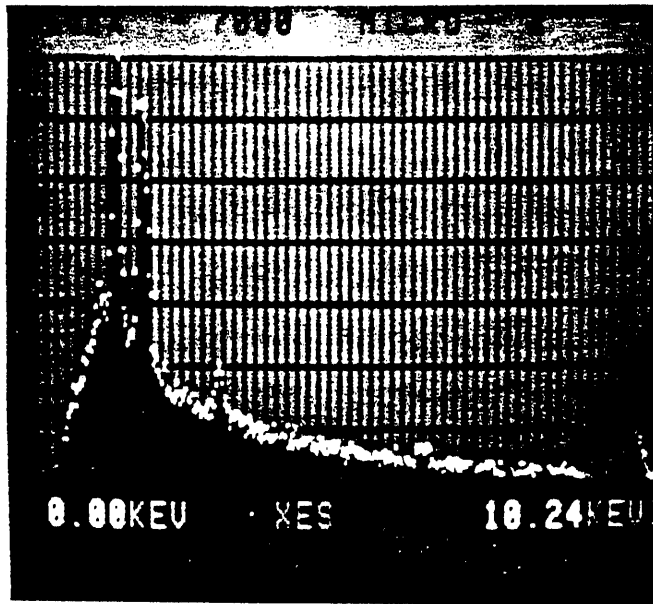
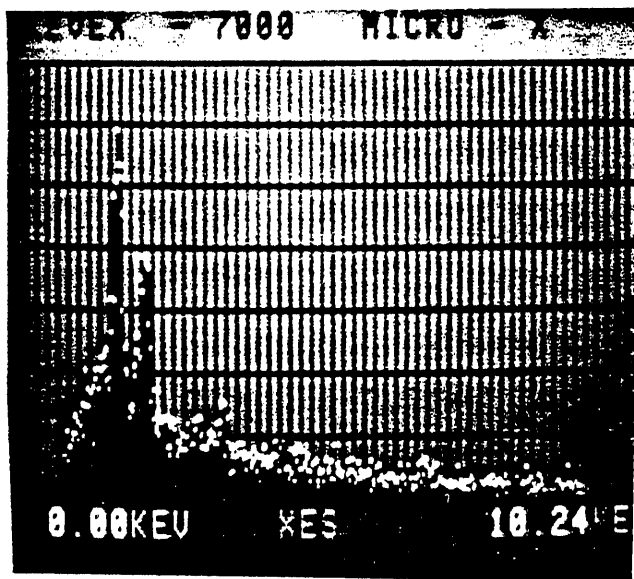


Figure 9: SEM Image resolution versus condenser lens setting



a. 11:00 (Bright) setting



b. 1:00 (Dim) setting

Figure 10: EDX spectra of a small graufilter glass particle on a carbon film at two condenser lens settings

GRAUFILTER

XRAY COUNTS vs DIAMETER

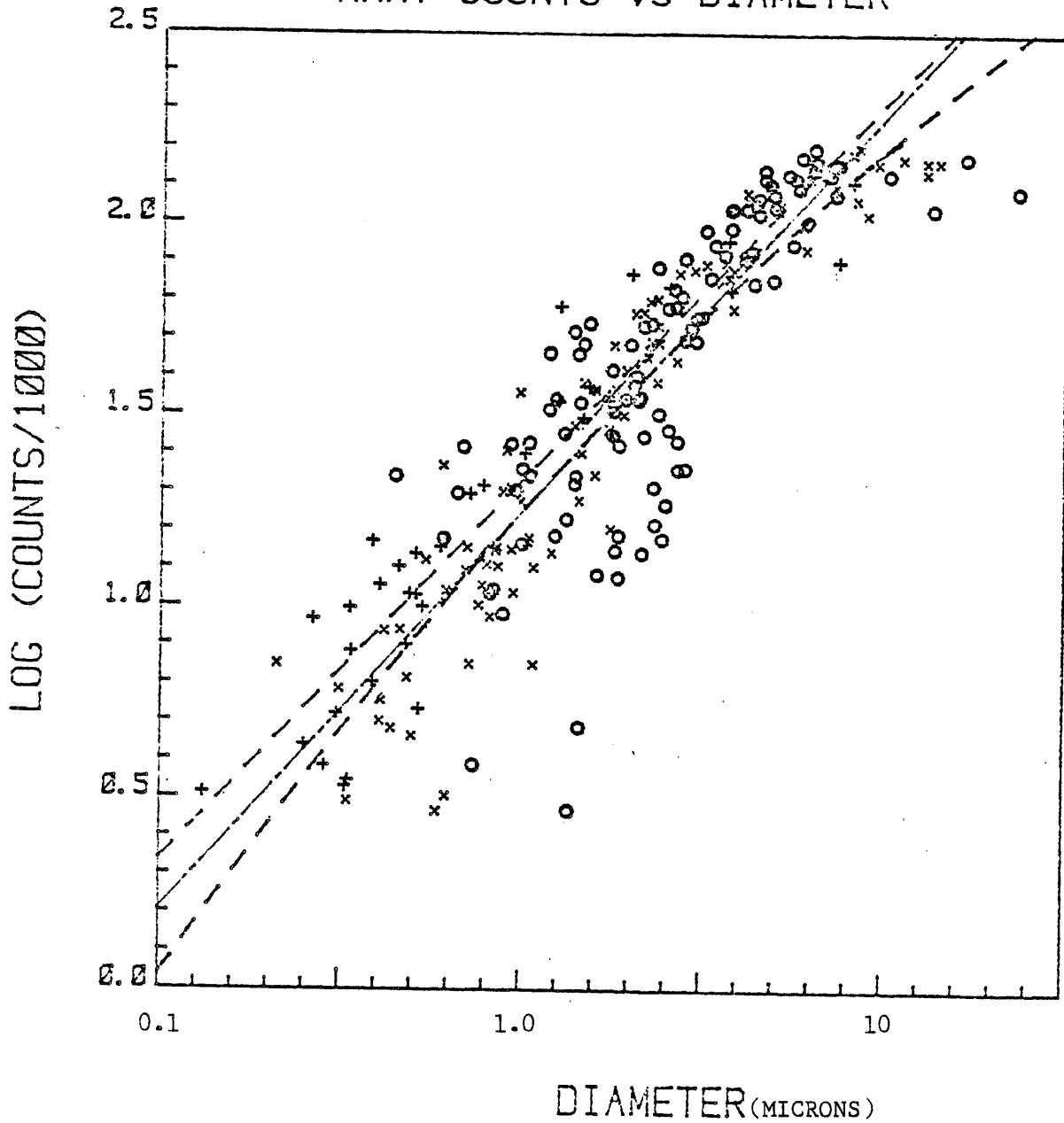
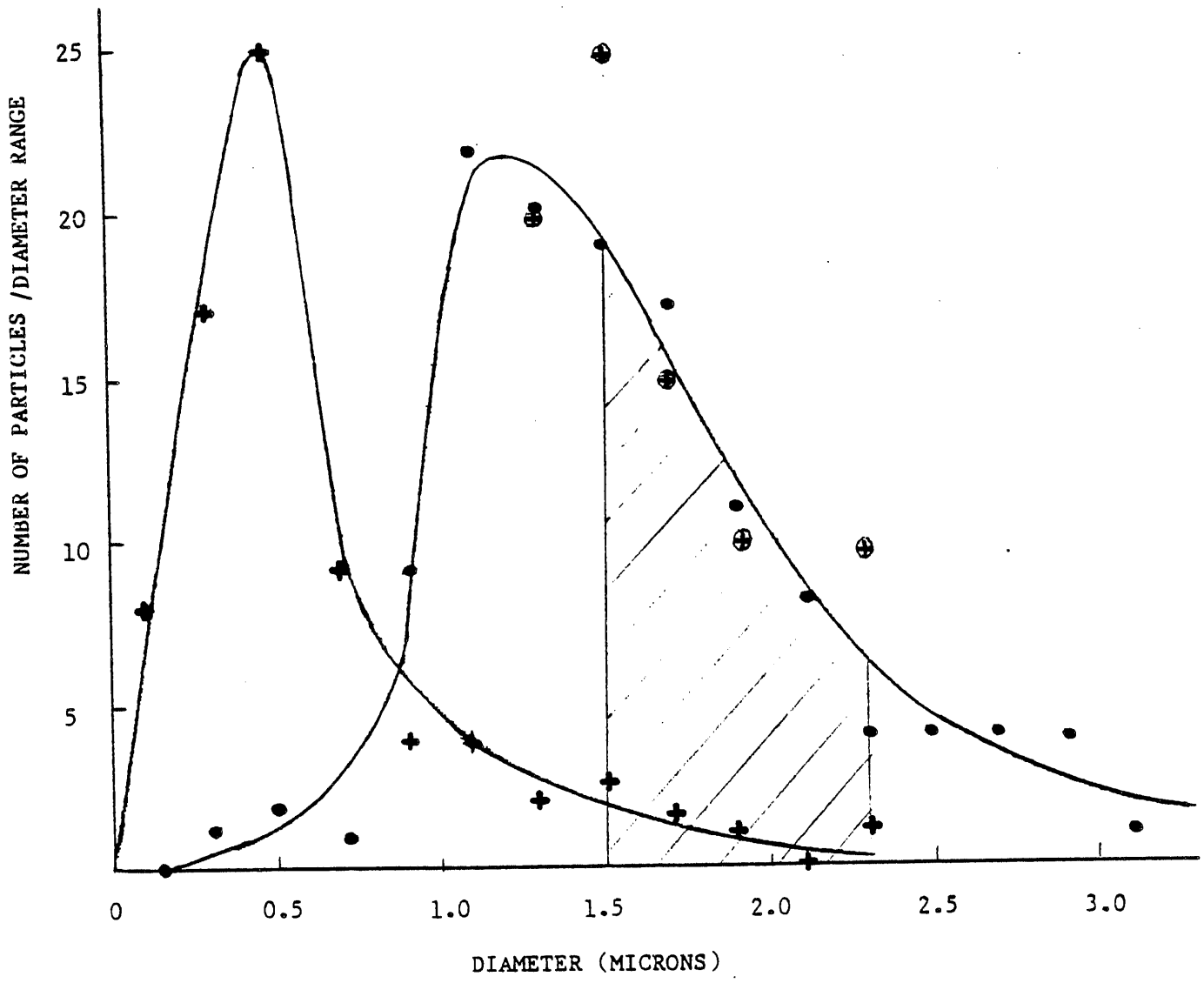


Figure 11: Plot of the logarithm of net peak x-ray counts versus the logarithm of particle diameter for graufilter glass

symbol		line	
+	2000X Magnification	— — — —	linear least-squares fit
x	400X Magnification	— — — —	linear least-squares fit
o	200X Magnification	— · — · —	(curved) quadratic least-squares fit



- 200X
- + 2000X
- ⊕ 2000X Scaled from shaded area

Figure 12: Size distributions of particles detected by APA at two different magnifications showing the overlap necessary for scaling (shaded).

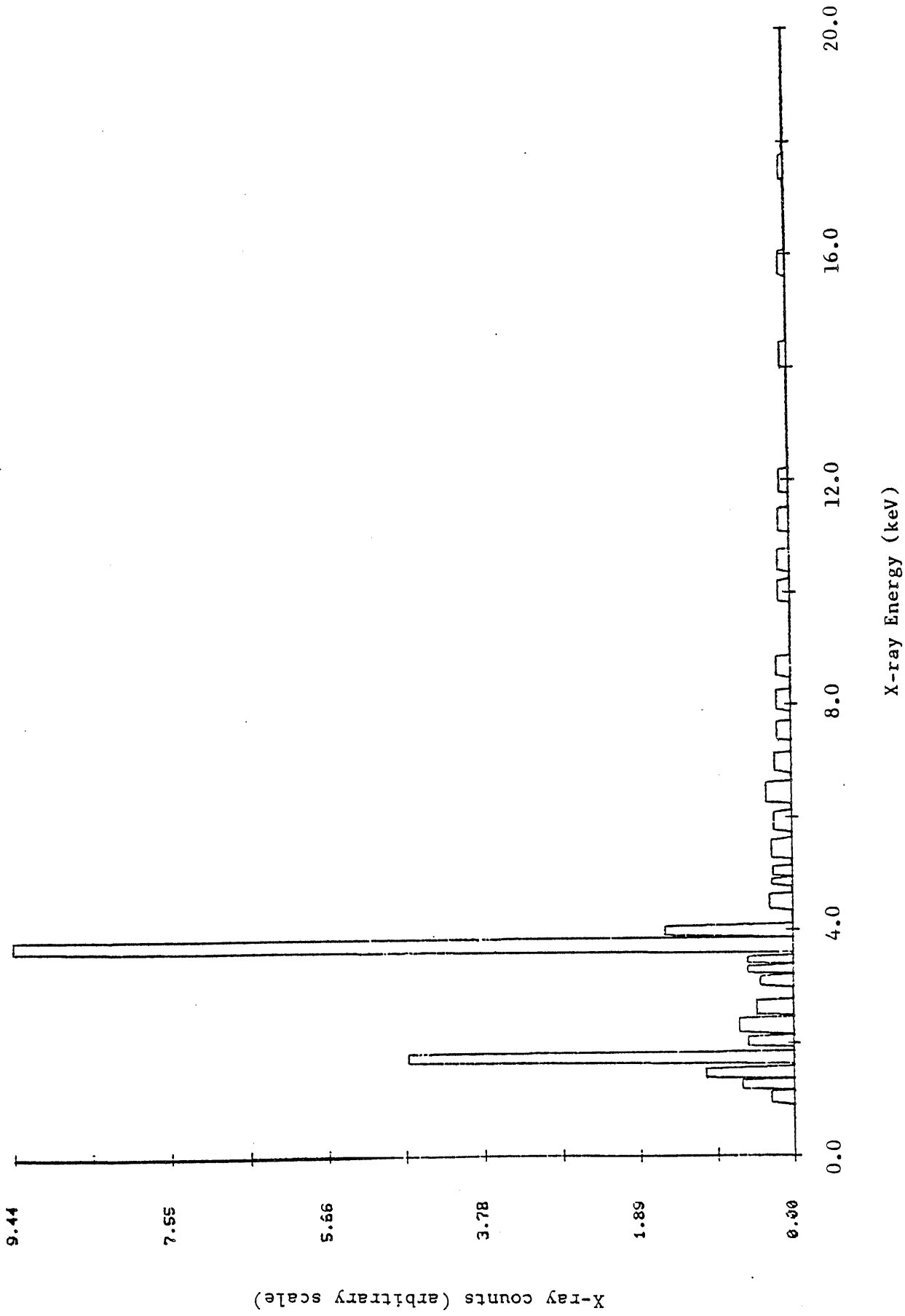


Figure 13: Elemental peak regions of clinker particle spectrum before background subtraction.

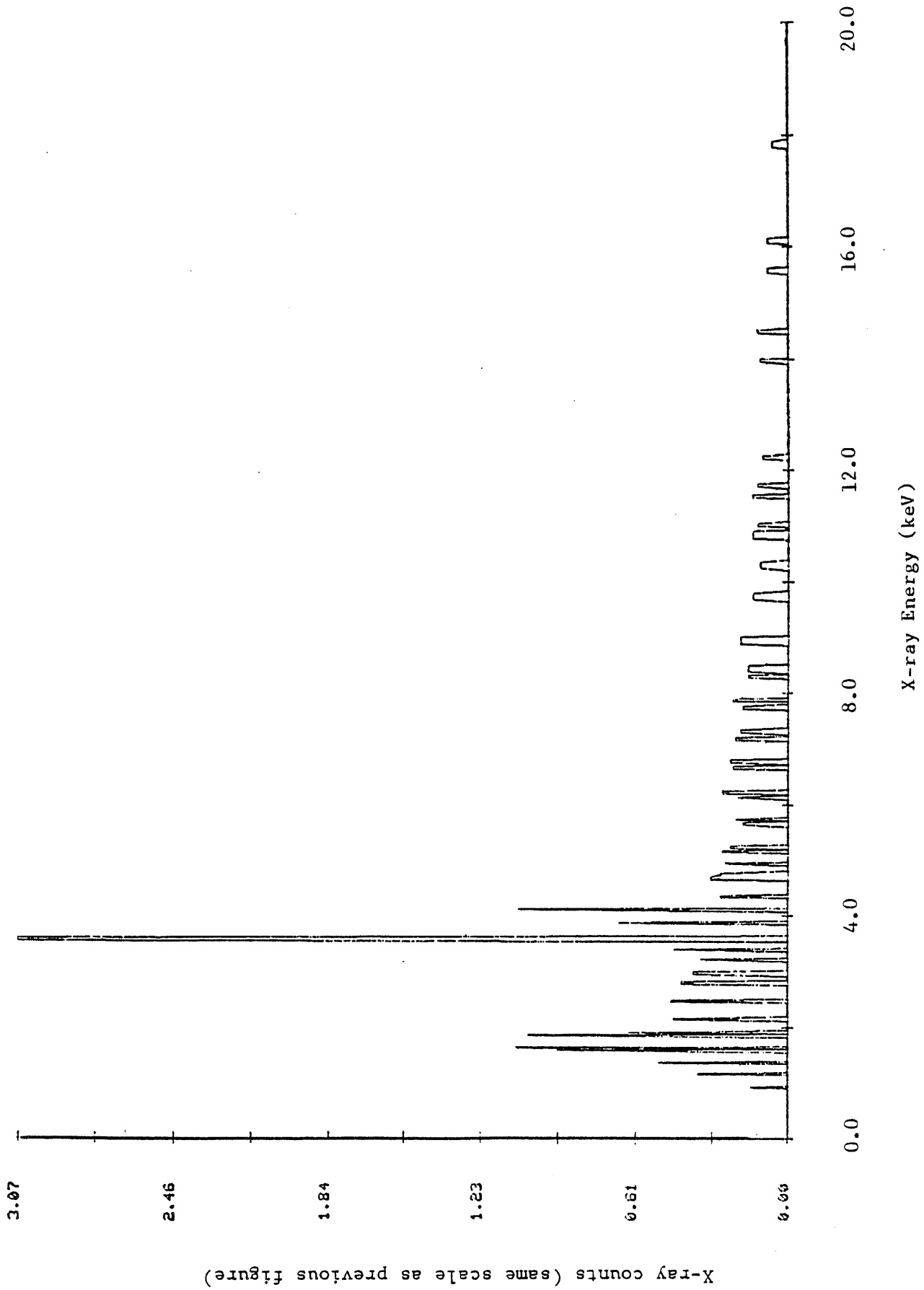


Figure 14: "Background" regions of clinker particle spectrum before interpolation, smoothing, and false peak removal.

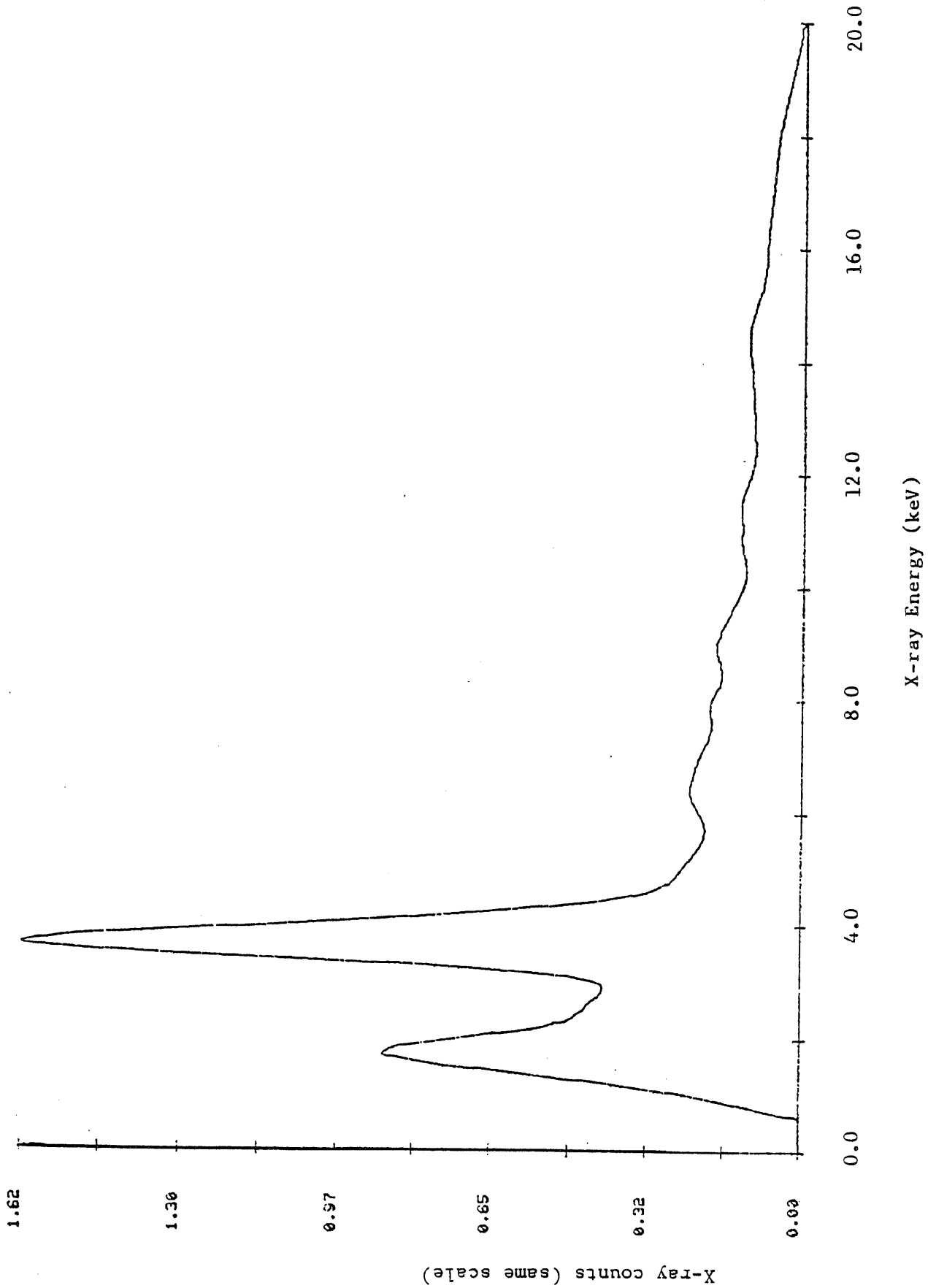


Figure 15: Smoothed, interpolated background spectrum of clinker particle before peak removal

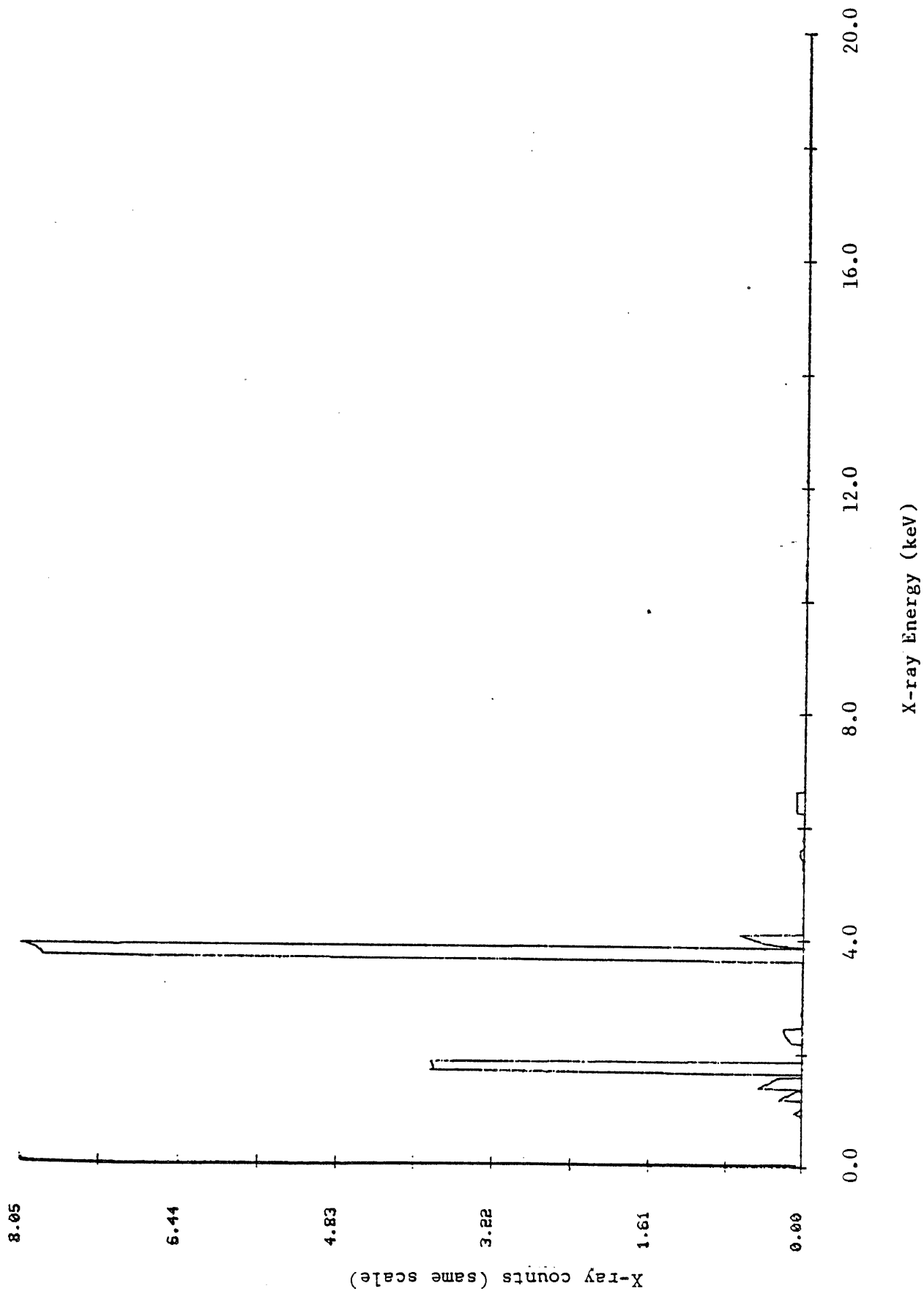


Figure 16: Net elemental peaks in clinker spectrum after subtraction of smoothed background (before removal of peaks from background)

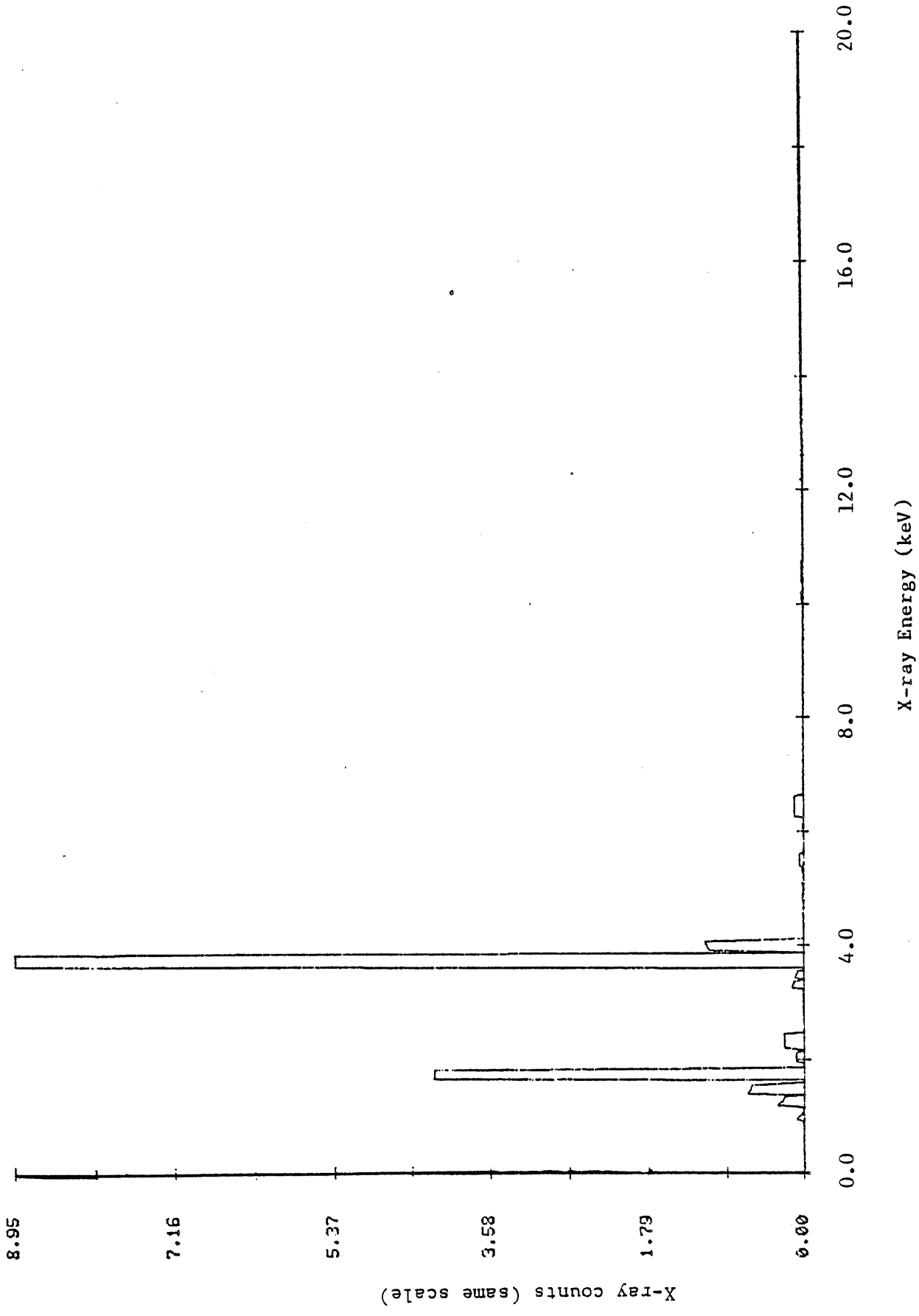


Figure 17: Net elemental peaks in clinker spectrum after subtraction of peak-corrected, smoothed background

POPULATION PERCENT VS. CHEMICAL CLASS

TYP	CLASS NAME	Z	0	1	2	3	4	5	6	7	8	9	0	1
			0	0	0	0	0	0	0	0	0	0	0	0
	MACR NO COUNTS	1.15E*												
	MACR COAL	0.00E												
	MACR LOW LOW COUNTS	0.00E												
	MACR LOW COUNTS	0.00E												
	MACR CLINKER	0.00E												
	MACR HCASIR CLINKER	0.00E												
	MACR LCASIR CLINKER	0.00E												
	MACR SHALE	0.00E												
	MACR SILICA	0.00E												
	MACR NACL-MARINE	0.00E												
	MACR LATERITE	1.15E*												
	MACR GYPSUM	0.00E												
	MACR LIMESTONE	0.00E												
	MACR CALCIUM	0.00E												
	MACR MG-TALC	0.00E												
	MACR ALUMINUM	0.00E												
	MACR KAOLINITE/ALSI	0.00E												
	MACR FELDSPAR	0.00E												
	MACR GLASS	0.00E												
	MACR ILLITE	0.00E												
	MACR MICA-VERMICULI	0.00E												
	MACR S/SO2/SO4	0.00E												
	MACR TiO2-PAINT	0.00E												
	MACR LEAD	0.00E												
	MACR CHLORIDES	0.00E												
	MACR IRON ORE	97.70E	*****											
	MACR IRON	0.00E												
	MACR COPPER	0.00E												
	MACR SODIUM	0.00E												
	MACR POTASSIUM	0.00E												
	MACR MISC SILICATE	0.00E												
	MACR MISCELLANEOUS:	0.00E												

Figure 19: Composition of iron ore source material by APA

POPULATION PERCENT VS. CHEMICAL CLASS

TYP	CLASS NAME	0	1	2	3	4	5	6	7	8	9
		0	0	0	0	0	0	0	0	0	0
	MACR NO COUNTS	0.24[
	MACR COAL	4.24[**									
	MACR LOW LOW COUNTS	0.00[
	MACR LOW COUNTS	0.00[
	MACR CLINKER	0.00[
	MACR HCASIR CLINKER	0.00[
	MACR LCASIR CLINKER	0.00[
	MACR SHALE	0.00[
	MACR SILICA	0.00[
	MACR NACL-MARINE	0.00[
	MACR LATERITE	82.82[*****									
	MACR GYPSUM	0.00[
	MACR LIMESTONE	0.00[
	MACR CAL EXUM	0.00[
	MACR MG-TALC	0.00[
	MACR ALUMINUM	0.00[
	MACR KAOLINITE/ALSI	0.00[
	MACR FELDSPAR	0.00[
	MACR GLASS	0.00[
	MACR ILLITE	1.41[*									
	MACR MICA-VERMICULI	0.00[
	MACR S/SO2/SO4	0.00[
	MACR TiO2-PAINT	0.47[
	MACR LEAD	0.00[
	MACR CHLORIDES	0.00[
	MACR IRON ORE	1.18[*									
	MACR IRON	6.59[***									
	*SUB SPHERES	2.59[+									
	MACR COPPER	0.00[
	MACR SODIUM	0.00[
	MACR POTASSIUM	0.00[
	MACR MISC SILICATE	0.24[
	MACR MISCELLANEOUS:	2.82[*									

Figure 20: Composition of laterite source material by APA

POPULATION PERCENT VS. CHEMICAL CLASS

TYP	CLASS NAME	%	0	1	2	3	4	5	6	7	8
			0	0	0	0	0	0	0	0	0
	MACR NO COUNTS	0.00E									
	MACR COAL	0.96E*									
	MACR LOW LOW COUNTS	0.00E									
	MACR LOW COUNTS	0.00E									
	MACR CLINKER	0.96E*									
	MACR HCASIR CLINKER	0.00E									
	MACR LCASIR CLINKER	0.00E									
	MACR SHALE	0.00E									
	MACR SILICA	0.48E									
	MACR NACL-MARINE	0.00E									
	MACR LATERITE	4.31E***									
	MACR GYPSUM	0.00E									
	MACR LIMESTONE	71.77E*****									
	MACR CALCIUM	11.96E*****									
	MACR MG-TALC	0.00E									
	MACR ALUMINUM	0.00E									
	MACR KAOLINITE/ALSI	0.00E									
	MACR FELDSPAR	0.00E									
	MACR GLASS	1.44E*									
	MACR ILLITE	0.00E									
	MACR MICA-VERMICULI	0.00E									
	MACR S/SO2/SO4	0.00E									
	MACR TiO2-PAINT	0.00E									
	MACR LEAD	0.00E									
	MACR CHLORIDES	0.00E									
	MACR IRON ORE	0.00E									
	MACR IRON	0.00E									
	MACR COPPER	0.00E									
	MACR SODIUM	0.00E									
	MACR POTASSIUM	0.00E									
	MACR MISC SILICATE	5.26E***									
	MACR MISCELLANEOUS:	2.87E**									

Figure 21: Composition of limestone source material by APA

POPULATION PERCENT VS. CHEMICAL CLASS

T/P	CLASS NAME	%	0	1	2	3	4	5
			0	0	0	0	0	0
	MACR NO COUNTS	0.33E						
	MACR COAL	2.32E**						
	MACR LOW LOW COUNTS	0.00E						
	MACR LOW COUNTS	0.00E						
	MACR CLINKER	0.00E						
	MACR HCASIR CLINKER	0.00E						
	MACR LCASIR CLINKER	0.00E						
	MACR SHALE	10.93E*****						
	MACR SILICA	43.05E*****						
	MACR NACL-MARINE	0.00E						
	MACR LATERITE	2.65E***						
	MACR GYPSUM	0.00E						
	MACR LIMESTONE	1.99E**						
	MACR CALCIUM	0.33E						
	MACR MG-TALC	0.00E						
	MACR ALUMINUM	0.00E						
	MACR KAOLINITE/ALSI	0.66E*						
	MACR FELDSPAR	0.00E						
	MACR GLASS	0.00E						
	MACR ILLITE	1.32E*						
	MACR MICA-VERMICULI	3.64E****						
	MACR S/SO2/SO4	0.00E						
	MACR TiO2-PAINT	0.00E						
	MACR LEAD	0.00E						
	MACR CHLORIDES	0.00E						
	MACR IRON ORE	0.00E						
	MACR IRON	0.00E						
	MACR COPPER	0.00E						
	MACR SODIUM	0.00E						
	MACR POTASSIUM	0.00E						
	MACR MISC SILICATE	30.13E*****						
	MACR MISCELLANEOUS:	2.65E***						

Figure 22: Composition of shale source material by APA

POPULATION PERCENT VS. CHEMICAL CLASS

TYP	CLASS NAME	%	0	1	2	3	4	5	6
			0	0	0	0	0	0	0
	MACR NO COUNTS	0.65[*]							
	MACR COAL	51.73[*****]							
	MACR LOW LOW COUNTS	0.00[
	MACR LOW COUNTS	0.00[
	MACR CLINKER	0.22[
	MACR HCASIR CLINKER	0.65[*]							
	MACR LCASIR CLINKER	0.43[
	MACR SHALE	0.87[*]							
	MACR SILICA	5.41[****]							
	MACR NACL-MARINE	0.00[
	MACR LATERITE	6.28[*****]							
	MACR GYPSUM	0.43[
	MACR LIMESTONE	4.11[***]							
	MACR CALCIUM	1.08[*]							
	MACR MG-TALC	0.00[
	MACR ALUMINUM	0.00[
	MACR KAOLINITE/ALSI	10.82[*****]							
	MACR FELDSPAR	0.00[
	MACR GLASS	0.00[
	MACR ILLITE	1.08[*]							
	MACR MICA-VERMICULI	0.43[
	MACR S/SO2/SO4	0.00[
	MACR TiO2-PAINT	0.22[
	MACR LEAD	0.00[
	MACR CHLORIDES	1.08[*]							
	MACR IRON ORE	5.63[*****]							
	MACR IRON	0.43[
	MACR COPPER	0.00[
	MACR SODIUM	0.00[
	MACR POTASSIUM	0.00[
	MACR MISC SILICATE	3.90[***]							
	MACR MISCELLANEOUS:	4.55[****]							

Figure 23: Composition of coal source material by APA

POPULATION PERCENT VS. CHEMICAL CLASS

TYP	CLASS NAME	Z	0	1	2
			0	0	0
MACR	NO COUNTS	10.71	[*****]		
MACR	COAL	11.81	[*****]		
MACR	LOW LOW COUNTS	0.00	[
MACR	LOW COUNTS	0.00	[
MACR	CLINKER	19.51	[*****]		
MACR	HCASIR CLINKER	12.09	[*****]		
MACR	LCASIR CLINKER	10.99	[*****]		
MACR	SHALE	0.27	[*		
MACR	SILICA	1.10	[***		
MACR	NACL-MARINE	0.00	[
MACR	LATERITE	1.37	[***		
MACR	GYPSUM	0.00	[
MACR	LIMESTONE	10.99	[*****]		
MACR	CALCIUM	5.49	[*****]		
MACR	MG-TALC	0.00	[
MACR	ALUMINUM	0.00	[
MACR	KAOLINITE/ALSI	0.27	[*		
MACR	FELDSPAR	0.00	[
MACR	GLASS	0.00	[
MACR	ILLITE	0.27	[*		
MACR	MICA-VERMICULI	0.55	[*		
MACR	S/SO2/SO4	0.00	[
MACR	TIO2-PAINT	0.55	[*		
MACR	LEAD	0.00	[
MACR	CHLORIDES	0.00	[
MACR	IRON ORE	0.82	[**		
MACR	IRON	0.82	[**		
SUB	SPHERES	0.27	[
MACR	COPPER	0.00	[
MACR	SODIUM	0.00	[
MACR	POTASSIUM	0.00	[
MACR	MISC SILICATE	4.12	[*****]		
MACR	MISCELLANEOUS:	8.24	[*****]		

Figure 24: Composition of clinker source material by APA

POPULATION PERCENT VS. CHEMICAL CLASS

TYP	CLASS NAME	Z	0	1	2	3	4
			0	0	0	0	0
	MACR NO COUNTS	0.00E					
	MACR COAL	0.00E					
	MACR LOW LOW COUNTS	0.00E					
	MACR LOW COUNTS	0.00E					
	MACR CLINKER	30.13E	*****				
	MACR HCASIR CLINKER	34.50E	*****				
	MACR LCASIR CLINKER	3.06E	****				
	MACR SHALE	0.00E					
	MACR SILICA	0.00E					
	MACR NACL-MARINE	0.00E					
	MACR LATERITE	0.44E	+				
	MACR GYPSUM	3.49E	****				
	MACR LIMESTONE	0.44E	+				
	MACR CALCIUM	1.31E	**				
	MACR MG-TALC	0.87E	+				
	MACR ALUMINUM	0.00E					
	MACR KAOLINITE/ALSI	0.00E					
	MACR FELDSPAR	0.00E					
	MACR GLASS	0.00E					
	MACR ILLITE	0.00E					
	MACR MICA-VERMICULI	0.00E					
	MACR S/SO2/SO4	0.00E					
	MACR TiO2-PAINT	0.00E					
	MACR LEAD	0.00E					
	MACR CHLORIDES	0.00E					
	MACR IRON ORE	0.00E					
	MACR IRON	0.00E					
	MACR COPPER	0.00E					
	MACR SODIUM	0.00E					
	MACR POTASSIUM	0.00E					
	MACR MISC SILICATE	0.00E					
	MACR MISCELLANEOUS:	25.76E	*****				

Figure 25: Composition of cement source material by APA

POPULATION PERCENT VS. CHEMICAL CLASS

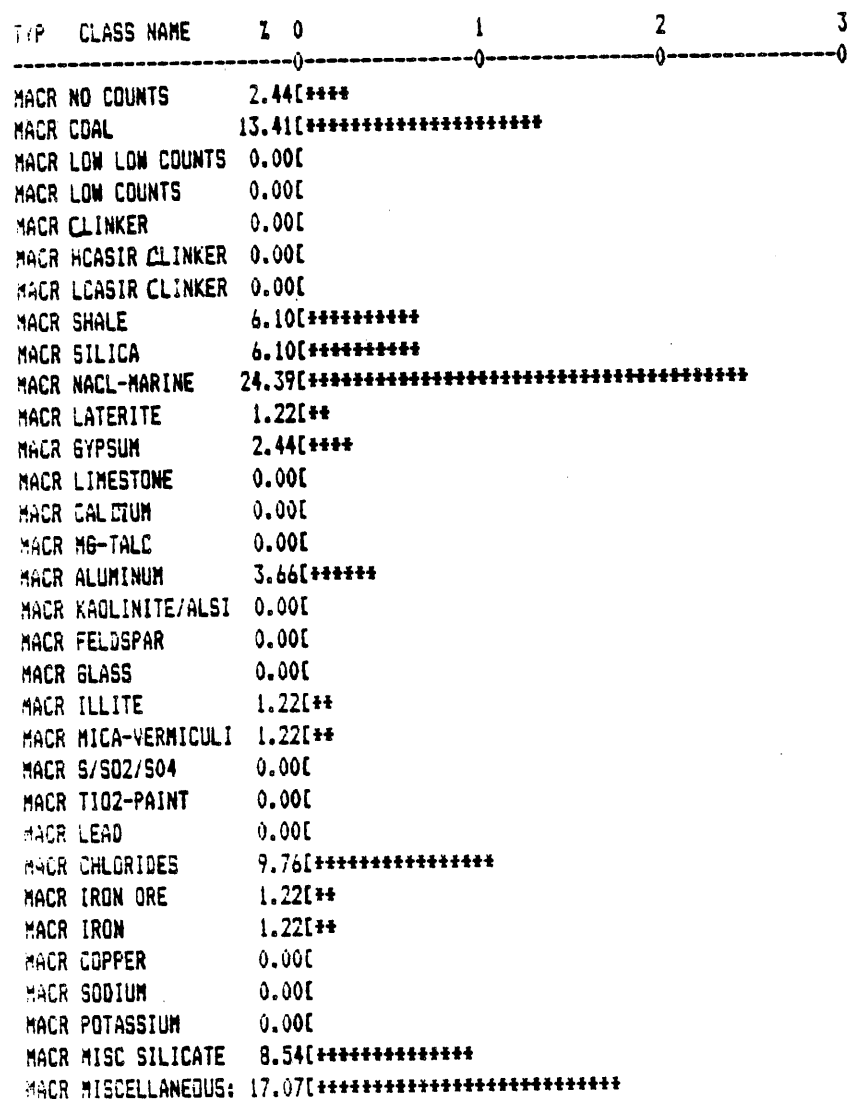


Figure 26: Composition of upwind aerosol (first sampling day) by APA

POPULATION PERCENT VS. CHEMICAL CLASS

TYP	CLASS NAME	%	0	1	2	3
			0	0	0	0
	MACR NO COUNTS	2.35	[****			
	MACR COAL	18.18	[*****			
	MACR LOW LOW COUNTS	0.00	[
	MACR LOW COUNTS	0.00	[
	MACR CLINKER	0.00	[
	MACR HCASIR CLINKER	0.00	[
	MACR LCASIR CLINKER	0.00	[
	MACR SHALE	6.16	[*****			
	MACR SILICA	4.11	[*****			
	MACR NACL-MARINE	27.27	[*****			
	MACR LATERITE	1.17	[**			
	MACR GYPSUM	2.64	[****			
	MACR LIMESTONE	0.00	[
	MACR CALCIUM	0.00	[
	MACR MG-TALC	0.00	[
	MACR ALUMINUM	0.00	[
	MACR KAOLINITE/ALSI	0.00	[
	MACR FELDSPAR	0.00	[
	MACR GLASS	0.88	[*			
	MACR ILLITE	3.52	[*****			
	MACR MICA-VERMICULI	3.81	[*****			
	MACR S/SO2/SO4	0.00	[
	MACR TIO2-PAINT	0.00	[
	MACR LEAD	0.00	[
	MACR CHLORIDES	9.09	[*****			
	MACR IRON ORE	0.00	[
	MACR IRON	0.29	[
	MACR COPPER	0.00	[
	MACR SODIUM	0.29	[
	MACR POTASSIUM	0.00	[
	MACR MISC SILICATE	12.32	[*****			
	MACR MISCELLANEOUS:	7.92	[*****			

Figure 27: Composition of upwind aerosol (second sampling day) by APA

POPULATION PERCENT VS. CHEMICAL CLASS

Typ	CLASS NAME	%	1	2
		0	0	0
	MACR NO COUNTS	0.00		
	MACR COAL	4.86[*****]		
	MACR LOW LOW COUNTS	0.00		
	MACR LOW COUNTS	0.00		
	MACR CLINKER	2.01[****]		
	MACR HCASIR CLINKER	2.51[*****]		
	MACR LCASIR CLINKER	1.51[****]		
	MACR SHALE	7.54[*****]		
	MACR SILICA	3.69[*****]		
	MACR NACL-MARINE	0.17		
	MACR LATERITE	17.42[*****]		
	MACR GYPSUM	2.18[****]		
	MACR LIMESTONE	6.53[*****]		
	MACR CALCIUM	5.19[*****]		
	MACR MG-TALC	0.00		
	MACR ALUMINUM	0.00		
	MACR KAOLINITE/ALSI	0.17		
	MACR FELDSPAR	0.00		
	MACR GLASS	0.34[*]		
	MACR ILLITE	4.02[*****]		
	MACR MICA-VERMICULI	3.35[*****]		
	MACR S/SO2/SO4	0.00		
	MACR TIO2-PAINT	0.34[*]		
	MACR LEAD	0.00		
	MACR CHLORIDES	1.34[***]		
	MACR IRON ORE	6.87[*****]		
	MACR IRON	3.18[*****]		
	*SUB SPHERES	1.34[***]		
	MACR COPPER	0.00		
	MACR SODIUM	0.00		
	MACR POTASSIUM	0.00		
	MACR MISC SILICATE	12.40[*****]		
	MACR MISCELLANEOUS:	14.41[*****]		

Figure 29: Composition of downwind aerosol (second sampling day) by APA

POPULATION PERCENT VS. CHEMICAL CLASS

TYP	CLASS NAME	%	0	1	2
MACR	NO COUNTS	0.12	[
MACR	COAL	4.93	[*****		
MACR	LOW LOW COUNTS	0.00	[
MACR	LOW COUNTS	0.00	[
MACR	CLINKER	1.72	[****		
MACR	LCASIR CLINKER	2.34	[*****		
MACR	LCASIR CLINKER	1.48	[****		
MACR	SHALE	8.37	[*****		
MACR	SILICA	3.45	[*****		
MACR	NACL-MARINE	0.12	[
MACR	LATERITE	16.75	[*****		
MACR	GYPSUM	2.09	[****		
MACR	LIMESTONE	6.03	[*****		
MACR	CALCIUM	5.42	[*****		
MACR	MG-TALC	0.00	[
MACR	ALUMINUM	0.00	[
MACR	KAOLINITE/ALSI	0.12	[
MACR	FELDSPAR	0.00	[
MACR	GLASS	0.25	[*		
MACR	ILLITE	3.33	[*****		
MACR	MICA-VERMICULI	3.20	[*****		
MACR	S/SO2/SO4	0.00	[
MACR	TIO2-PAINT	0.25	[*		
MACR	LEAD	0.00	[
MACR	CHLORIDES	1.23	[***		
MACR	IRON ORE	8.00	[*****		
MACR	IRON	3.08	[*****		
+SUB	SPHERES	1.23	[***		
MACR	COPPER	0.00	[
MACR	SODIUM	0.00	[
MACR	POTASSIUM	0.00	[
MACR	MISC SILICATE	12.19	[*****		
MACR	MISCELLANEOUS	15.52	[*****		

Figure 30: Composition of downwind aerosol (second sampling day - duplicate filter section) by APA